Center for Alternative Fuels, Engines & Emissions

West Virginia University

FINAL REPORT

Contract No. 07-340

Testing of Volatile and Nonvolatile Emissions from Advanced Technology Natural Gas Vehicles

Principal Investigator:
Mridul Gautam, Ph.D.
mgautam@mail.wvu.edu
Department of Mechanical and Aerospace Engineering
West Virginia University
Morgantown, WV 26506

Co-Principal Investigators:
Arvind Thiruvengadam, Daniel Carder, Marc C. Besch, Benjamin Shade,
Greg Thompson, Nigel Clark

Prepared for:
John Collins
Project Officer
State of California Air Resources Board
Research Division
PO Box 2815
Sacramento, CA 95812
E-mail: jcollins@arb.ca.gov

Prepared by:

West Virginia University Research Corporation
886 Chestnut Ridge Road
West Virginia University
Morgantown, WV 26506

July, 2011

EXECUTIVE SUMMARY

Natural gas vehicles have proved to be an economic alternative to meet USEPA emissions regulation. In particular the 3-way oxidation catalyst equipped, 2010 emissions compliant stoichiometric heavy-duty natural gas engines have proven to be a viable alternative in comparison to SCR equipped heavy-duty diesel engines. Stoichiometric natural gas engine technology is capable of meeting the stringent PM and NO_x standards with only a 3-way oxidation catalyst as its exhaust after-treatment system. However, lack of sufficient data and literature on the exhaust emissions from advanced natural gas engines and the potential adverse health effects has raised concern amongst regulatory agencies.

This CARB funded study focuses primarily on characterizing the toxicity of the volatile fraction of PM from advanced heavy-duty natural gas engines. The objective of the study also includes characterizing the unregulated species of the exhaust together with number concentration and size distribution of ultrafine nanoparticle emissions. The work plan involved the chassis dynamometer testing of two heavy-duty natural gas transit buses that are compliant with the USEPA 2010 emissions regulation. Since the project was focused at investigating the effect of volatility on toxicity, the test procedure included a thermal denuder to remove the volatile component prior to collection on the filters.

ARB is conducting toxicity related assays of samples collected in this test program, and will provide those data as an addendum to this report.

TABLE OF CONTENTS

EXECUTIVE SUMMARY **2**

LIST OF FIGURES **5**

LIST OF TABLES **7**

1 INTRODUCTION **8**

1.1 OBJECTIVE 8

2 REVIEW OF BACKGROUND STUDIES **9**

2.1 PM EMISSIONS AND HEALTH EFFECTS 9
2.2 LUBRICATION OIL CONSUMPTION AND PM EMISSIONS IN GAS-FUELED ENGINES 14
2.3 AMMONIA EMISSIONS FROM NATURAL GAS ENGINES WITH THREE-WAY CATALYST 17
2.4 AMMONIA EMISSION MEASUREMENT TECHNIQUES 18

3 EXPERIMENTAL SETUP **23**

3.1 VEHICLE EMISSIONS TESTING LABORATORY 23
3.1.1 Chassis Dynamometer *23*
3.1.2 Emissions Measurement Container *26*
3.1.2.1 Gaseous Emissions Sampling System 28
3.1.2.2 PM Sampling and Measurement System 28
3.1.2.3 CVS Flow Control 30
3.2 TEST VEHICLE AND ENGINE SPECIFICATIONS 30
3.3 TEST CYCLE 31
3.4 THERMODENUDER PM SAMPLING SYSTEM 32
3.5 AMMONIA MEASUREMENT SYSTEM 34
3.6 PARTICULATE MATTER SIZING SETUP 34
3.7 UNREGULATED EMISSIONS SAMPLING SYSTEM 35
3.7.1 Carbonyls *36*
3.7.2 Polycyclic Aromatic Hydrocarbon (PAH/n-PAH) Sampling System *36*
3.7.3 VOC Canister Sampling System *37*
3.7.4 Cyclonic Particle Classifier *37*
3.7.5 Gas Bag Sampling *37*
3.8 INSTRUMENTATION CONTROL AND DATA ACQUISITION 37
3.9 MEDIA 38
3.10 MEDIA CONDITIONING AND WEIGHING 38
3.11 MEDIA SHIPPING AND TRACKING 39

4 EMISSIONS TESTING PROCEDURE **40**

4.1 SET-UP 40
4.2 LABORATORY CHECKS 40
4.3 MASS FLOW CONTROLLER CALIBRATION 41
4.4 CVS-SSV DILUTION TUNNEL VERIFICATION 42
4.5 TEST PROCEDURE 43
4.6 EMISSIONS CALCULATIONS 46
4.6.1 Equations to Calculate Distance Specific Mass of Exhaust Species *46*
4.6.1.1 Volatile Organic Hydrocarbons 47
4.6.1.2 Semi Volatile and Particle Bound Hydrocarbon Analysis 47

5 RESULTS AND DISCUSSIONS 48

5.1 REGULATED EMISSIONS 48
5.2 CRITERIA POLLUTANT COMPARISON WITH PREVIOUS STUDIES 51
5.3 UNREGULATED EMISSIONS 52
5.3.1 Poly aromatic Hydrocarbons (PAH) Emissions 52
5.3.2 Elemental Carbon / Organic Carbon (EC/OC) 54
5.3.3 Volatile Organic Compounds (VOC) 56
5.3.4 Carbonyl Emissions 58
5.3.5 Water Soluble Ions Emissions 59
5.3.6 Metals Emissions 60
5.3.7 Particle Size Distribution and Concentration 61
5.3.8 Ammonia emissions 65

6 CONCLUSIONS 69

7 REFERENCES 70

LIST OF FIGURES

Figure 1 Solvent extract of soot collected from a single-cylinder Proteus engine: Bacterial mutagenicity as a function of engine speed, load, and fuel type. *12*
Figure 2 Components of a Chassis Dynamometer *24*
Figure 3 Connecting and supporting structure of chassis dynamometer *25*
Figure 4 Schematic of the transportable laboratory container *27*
Figure 5 View of the transportable laboratory container *27*
Figure 6 Schematic of the PM sampling system *29*
Figure 7 1065 compliant PM sampling system on-board the transportable laboratory container *29*
Figure 8 Speed vs. Time trace of triple-UDDS cycle *32*
Figure 9 Outside view of thermodenuder sampling system. *33*
Figure 10 Inside view of thermodenuder sampling system *33*
Figure 11 Schematic of DRI's PUF/XAD cartridge housing *36*
Figure 12 CVS and media sampling setup *45*
Figure 13 Work specific regulated emissions summary of test vehicles over the different test cycles *49*
Figure 14 Distance specific regulated emissions summary of test vehicles over different cycles *50*
Figure 15 Cruise mode criteria pollutant comparison between current and previous studies *51*
Figure 16 Distance specific (time-specific for Idle) PAH emissions results of CNG bus 1 ..... *53*
Figure 17 Distance specific (time-specific for Idle) PAH emissions results of CNG bus 2 ..... *54*
Figure 18 Distance specific EC/OC emissions results of bus 1 ..... *55*
Figure 19 Distance specific EC/OC emissions results of bus 2 ..... *56*
Figure 20 Distance specific BTEX emissions results from bus 1 and bus 2 ..... *57*
Figure 21 Distance specific VOC emissions of bus 1 and bus 2 ..... *58*
Figure 22 Distance specific (time-specific for Idle) Carbonyl emissions results of CNG bus 1 and 2 ..... *59*
Figure 23 Distance specific (time-specific for Idle) water soluble ions emissions results of CNG bus 1 and 2 ..... *60*
Figure 24 Distance specific (time-specific for Idle) metals emissions results of CNG bus 1 and 2 ..... *61*
Figure 25 Average PM Concentration over triple-UDDS cycle, Sampled from CVS tunnel, No dilution ratio corrections, EEPS *62*
Figure 26 Average PM Concentration over 45Mph steady-state mode (60min), Sampled from CVS tunnel, No dilution ratio corrections, EEPS *63*
Figure 27 Average PM Concentration over Idle mode (30min), Sampled from CVS tunnel, No dilution ratio corrections, EEPS *64*
Figure 28 Non-denuded toxicity filters sampled during idle mode operation *65*
Figure 29 Thermally denuded toxicity filters sampled during idle mode operation *65*
Figure 30 Total PM Concentration over Idle mode, Sampled from CVS tunnel, No dilution ratio corrections, EEPS *65*

Figure 31 Ammonia concentrations over 30 MPH steady state 66
Figure 32 Ammonia concentrations over 45 MPH steady state 67
Figure 33 Ammonia concentrations over UDDS.....67

LIST OF TABLES

Table 1 Test vehicle specifications 31
Table 2 Test vehicle power train specifications 31
Table 3 List of species and sample media 38
Table 4 Gaseous and PM measurement system verification checks 40
Table 5 Analyzer verification checks 41
Table 6 Cycle repetitions for PM mass loading 44
Table 7 Summary of sampling media, sampling device and methods used to analyze unregulated exhaust species 45

1 INTRODUCTION

Heavy-duty natural gas engines compliant with the 2010 EPA emissions standards have a clear advantage over diesel engines in meeting regulations with minimal after-treatment configuration. The stoichiometric Cummins ISLG engines employ only a three-way oxidation catalyst to meet the 0.20 g/bhp-hr NO_x emissions standards. Heavy-duty natural gas engines are largely promoted as a cleaner burning engine with respect to low PM mass emissions. However, lack of sufficient data and literature on the exhaust emissions from advanced natural gas engines and the potential adverse health effects has raised concern amongst regulatory agencies.

1.1 OBJECTIVE

The primary objective of this study is to characterize the toxicity of the volatile fraction of PM from advanced heavy-duty natural gas engines. The primary objective is to be achieved by performing a complete chemical characterization of the exhaust, which includes sampling and analysis of unregulated species in the vehicle exhaust together with particle number concentration and size distribution measurements of the diluted exhaust. Also, one of the key specific objectives of this study is to separately collect the volatile and the non-volatile component of the PM through use of thermodenuders. The collected samples would be further analyzed for toxicity and mutagenicity assays to investigate the difference in toxicity profile of volatile and non-volatile component of PM.

2 REVIEW OF BACKGROUND STUDIES

It is presumed that the CNG-fueled vehicles produce PM emission-free exhaust streams. However, work by Gautam et al. [1] and Kappanna [2] have shown that while the mass emissions of PM from CNG-fueled vehicles may be an order of magnitude lower than comparable diesel vehicles, PM emissions on a number-count basis from a CNG vehicle without an exhaust after-treatment may be significantly higher. Further, on a mass-basis PM emissions from a CNG vehicle without an exhaust after-treatment system may be of the same order as those from trap-equipped diesel engines.

2.1 PM EMISSIONS AND HEALTH EFFECTS

Concerns about potential health effects from inhalation of vehicle emissions have increased as the result of epidemiological studies showing increased morbidity and mortality in people exposed to air pollutants [3]. Based on reviews of the published literature, the National Institute for Occupational Safety and Health (NIOSH) [4], the International Agency for Research on Cancer (IARC) [5], and the US Environmental protection Agency (USEPA) [6], have declared diesel exhaust a potential or probable human carcinogen. There is very limited published work on the characterization of CNG-fueled engine exhaust emissions [1, 7, 8, 9, 10, 11, 12, 13 and 14] and virtually none of those studies address the size-segregated volatility of UF particles, and the potential health risks associated with CNG fueled engine exhaust emissions. Controlled human exposure studies of diesel exhaust or diesel exhaust particulate matter (PM) have shown inflammatory responses or alterations in immune responses [15, 16, 17, 18, 19 and 20]. Further, Brauer et al. [21], Brunekreef et al. [22], and Finkelstein [23] have shown that health effects are inversely correlated with distance from major highways.

To counter the potential adverse health effects of diesel exhaust emissions, compressed natural gas (CNG) has been promoted as a cleaner-burning fuel. In fact, CNG-fueled heavy duty vehicles appear to produce less PM, but greater total hydrocarbons compared to diesel-fueled vehicles [24]. Characterization of the emissions from such vehicles has demonstrated that the emissions contain potentially toxic materials [25]. However, to date, few of the biological effects of these emissions have been examined and/or published. Despite the lack of toxicological data, portions of some heavy-duty vehicle fleets have been converted to CNG [7, 20].

Published literature on toxicity of nanoparticle emissions from CNG fueled vehicles is woefully lacking. A number of factors are likely to influence the toxicity of nanoparticles. These include

1. Particle number and size
2. Surface dose
3. Surface coatings on particles
4. The degree to which ambient ultrafine particles "age" and become aggregates, due in large part to surface characteristics
5. Surface charges on particles, as well as particle shape and/or electrostatic attraction potential
6. Particle chemistry

A few studies have measured the volatility of PM in dynamometer tests using tandem differential mobility analyzer (TDMA) systems [26]. The volatility measurements yield information on particle mixing characteristics and nanoparticle vapor pressures, which can be compared with standards to estimate the carbon numbers of organic components. Given that inhalation and deposition behavior of nanoparticles is determined by particle mobility rather than aerodynamic properties, mobility based measurements are especially well-suited to nanoparticle studies related to health effects.

Ayala et al. [7] conducted size-resolved PM mass and number emission measurements on diesel and CNG buses. Ames mutagenicity assays were conducted on extracts from diesel and CNG total PM samples. It was reported that tailpipe emission samples from a compressed natural gas (CNG)-fueled transit bus without an after-treatment system had measurable levels of toxic compounds such as formaldehyde (HCHO), nanoparticles (<50 nm) and mutagenic emissions Ames assay. These emissions levels, in some cases were greater than those of a comparable diesel transit bus equipped with an exhaust after-treatment device and fueled by ultra-low sulfur diesel (ULSD). In another study, Holmen et al. [13] compared the submicron particle size distributions using simultaneous SMPS measurements under two dilution conditions, a minidiluter and the legislated constant volume sampler (CVS) from a compressed natural gas CNG -fueled and diesel particulate filter (DPF) -equipped diesel configurations to conventional diesel engines. In another study, Ayala et al. [8] investigated the effect of oxidation catalyst on CNG transit bus emissions.

The current knowledge base woefully lacks data that directly links the physical and chemical characteristics of specific exhaust emissions species, or a combination of species to health risks, and how such health risks change as a function of changes in the composition of exhaust emissions. Moreover, except for bioassay-directed fractionation schemes that have identified nitro-polycyclic aromatic hydrocarbons as major drivers of bacterial mutagenicity, few approaches have been used to determine the chemical species driving the health hazards of complex emissions [27].

Liu et al. [28] performed three measures of genotoxic activity on solvent extracts of diesel and gasoline engine exhaust particulate matter (PM) and vapor-phase semi-volatile organic compounds (SVOC's), as part of a US Department of Energy multi-institutional study of the exhaust toxicities of modem gasoline, diesel, and natural-gas mobile vehicle engines [29, 30, 31]. Acetone extracts of engine exhaust particulate matter (PM) and vapor-phase semi-volatile organic compounds (SVOC's) collected from a set of 1998-2000 model year normal emitter diesel engine automobile or light truck vehicles and from a set of 1982-1996 model year normal emitter spark-ignition gasoline engine automobiles or light truck vehicles were assayed for in vitro genotoxicity. When normalized for response in terms of mileage, diesel exhaust PM extract was 3- to 7-fold higher for mutagenic activity than gasoline exhaust PM. Gasoline exhaust SVOC extract expressed higher mutagenicity than diesel SVOC extract on an extracted-mass basis, with diesel SVOC 2- to 3- times the more active on a mileage basis. Gasoline engine PM extract and SVOC extract both gave positive dose-response relationships for micronucleus induction. Diesel PM extract expressed chromosomal damage, which was about one-tenth that of gasoline PM on a mass of extract basis, but was comparably active on a mileage basis. Diesel exhaust SVOC extract was inactive for micronucleus induction in V79 cells. Gasoline exhaust PM extract was positive in the single cell gel electrophoresis (SCGE) assay for DNA damage; diesel exhaust PM extract was active at the higher doses. Gasoline exhaust SVOC extract was active for DNA damage at lower doses with toxicity preventing measurement at higher doses, while diesel exhaust SVOC extract was inactive at all but the highest dose with no positive dose-response.

McMillian et al. [32] measured bacterial gene mutation activity for the organic solvent extract of diesel exhaust particulate material generated by a single-cylinder diesel engine operated over 7 steady-state modes (key-states) using Fischer-Tropsch fuel synthesized from

natural gas and using conventional federal diesel No. 2 fuel. A significant difference in mutagenic activity between fuel type and key state as well as strain and activation type was indicated. From an interaction perspective, the difference among key states was consistent across fuel types. Within key states the effect of speed x load interaction was significant, as was the effect of load in general. There was significant curvature in the speed effect (the quadratic term was significant). A quadratic response surface was developed, which correlated mutagenic activity with engine speed and load for each fuel type. The results graphically demonstrate that there is no single level of genotoxicant activity for diesel exhaust PM extract. It was reported that bacterial gene mutation activity is a strong function of engine operation for this engine and fuel types (see Figure 1). Also, particles larger than (100 nm) display a higher mutagenic activity compared to smaller particles (smaller than 100 nm).

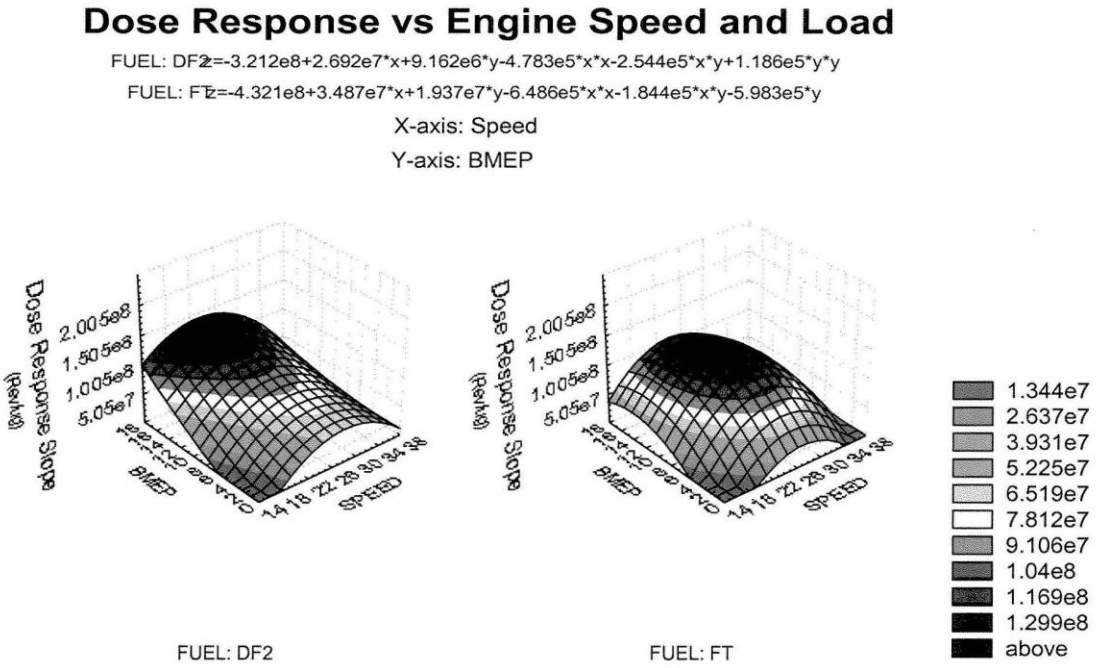

Figure 1 Solvent extract of soot collected from a single-cylinder Proteus engine: Bacterial mutagenicity as a function of engine speed, load, and fuel type.

Bagley, et al. [33], studied the characterization of fuel and after-treatment devices effects on diesel emissions. They found that the use of an oxidation catalyst in combination with a PM trap substantially decreased the number of particles and the mutagenic activity. Yuan et al. [34], studied the mutagenic activity from emissions from gasoline engines using leaded and unleaded gasoline. The results show that both types of gasoline can induce mutation in the Salmonella test

strain TA98 and TA100. Furthermore they reported that mutagenic activity decreased when the metabolic activator was used.

Okamoto et al. [35] performed mutagenic test on the exhaust from transit buses operating on CNG. The study reported a lower mutagenic activity on buses equipped with oxidation catalyst, compared to buses without oxidation catalyst. The study also concluded that the mutagenic activity was higher without the metabolic activator. Kado et al. [36] reported similar results for transit buses operated on CNG, but also reported results using the tester strain TA98NR, which is insensitive to certain types of nitro-PAH. In this study they found that the mutagenic activity using the TA98NR decreased, indicating the possible presence of nitro-PAH in the PM emissions.

Seagrave et al. [20] investigated the composition, toxicity, and mutagenicity of particulate matter (PM) and semivolatile emissions from heavy-duty compressed natural gas-powered vehicles. Authors sampled particulate matter and vapor-phase semivolatile organic compounds (SVOC) from three buses fueled by compressed natural gas. The bus engines included a well-functioning, conventional engine; a "high emitter" engine; and a new technology engine with an oxidation catalyst. Chemical analysis of the emissions showed differences among these samples, with the high emitter sample containing markers of engine oil constituents. PM + SVOC samples were also collected for mutagenicity and toxicity testing. Extraction efficiencies from the collection media were lower than for similarly collected samples from gasoline or diesel vehicles. Responses to the recovered samples were compared on the basis of exhaust volume, to incorporate the emission rates into the potency factors. Mutagenicity was assessed by Salmonella reverse mutation assay. Mutagenicity was greatest for the high emitter sample and lowest for the new technology sample. Metabolic activation reduced mutagenicity in strain TA100, but not TA98. Toxicity, including inflammation, cytotoxicity, and parenchymal changes, was assessed 24h after intra-tracheal instillation into rat lungs. Lung responses were generally mild, with little difference between the responses to equivalent volumes of emissions from the normal emitter and the new technology, but greater responses for the high emitter. These emission sample potencies were further compared on the basis of recovered mass with previously reported samples from normal and high-emitter gasoline and diesel vehicles. While mutagenic potencies for the CNG emission samples were similar to the range observed in the gasoline and diesel

emission samples, lung toxicity potency factors were generally lower than those for the gasoline and diesel samples.

McDonald et al. [27], investigated the statistical relationship between particle and semivolatile organic chemical constituents in gasoline and diesel vehicle exhaust samples, and toxicity as measured by inflammation and tissue damage in rat lungs and mutagenicity in bacteria. It was concluded that specific nitro-polycyclic aromatic hydrocarbons, which are important for mutagenicity were not related to lung toxicity, which was associated with organic carbon and select organic compounds that are present in lubricating oil.

2.2 LUBRICATION OIL CONSUMPTION AND PM EMISSIONS IN GAS-FUELED ENGINES

The PM generated by internal combustion engines originates from fuel and lubrication oil consumption. In gas-fueled engines, in general, and hydrogen fueled engines, in particular, the only source of PM is the lubrication oil, [37]. PM is basically composed of organic carbon (OC), elemental carbon (EC), and metallic ash. The following classification is given by Lee et al. [38], for the particulate matter based on the hydrogen to carbon ratio; for organic carbon (H/C> 1), and for elemental carbon (H/C < 1). Miller et al. [39], found that in a hydrogen engine the PM was mostly composed of metallic ash, from the lubrication oil additives. Miller also concluded that most of the carbon in the PM was in the OC form. CNG - fueled heavy-duty engines show similar characteristics [1, 7, 8, 9, 10, 11, 12, 13 and 14].

An understanding of a link between specific exhaust emissions species PM-bound, in particular, and the origin of such species as a function of engine technology, and engine operation is critical for developing technological solutions to mitigate health effects of engine emissions.

Immediately downstream of the exhaust manifold all particles are mainly composed of carbonaceous particles (soot), and metallic ash. As the exhaust cools, soluble organic compounds (SOP) condense and adsorb to the surfaces of carbonaceous particles or nucleate to form nanoparticles (less than 50 nanometers). Further downstream, the agglomeration process decreases the number of particles, but does not affect the total mass. The nucleation process increases the number of particles, but does not affect the total mass. Kittelson and Abdul Khalek, [40] found that the formation of nanoparticles was affected by the amount of soot in the exhaust stream. As the soot mass increased the number of nanoparticles decreased. Lack of carbonaceous

soot particles and the presences of lube-oil (heavy-organics) based nanoparticles are very characteristic of CNG-fueled engine exhaust steam. This was attributed to the adsorption of organic compounds onto the surface of soot particles as well as greater probability of particle-particle interaction and agglomeration. Based upon Ames-mutagenicity assays on size-fractionated PM samples, McMillian et al. [32] had reported that particles larger than 100 nm displayed higher mutagenic activity compared to particles smaller than 100 nm.

It is well recognized that a considerable amount of the SOF is derived from the lubrication oil. Oil transport through the ring pack in the latter part of the expansion and exhaust stroke is exposed to lower temperature combustion gases, which reduces the oxidation amount, and increases the lubrication oil contribution to SOF. Froelund and Yilmaz [41] reported that 30 percent of the total lubrication oil evaporation occurs late part of the expansion and exhaust strokes, which increases the contribution to SOF. Andersson et al. [42] reported that nucleation of particles increased during engine deceleration. This could be attributed to a lower gas temperature inside the combustion chamber reducing the lubrication oil oxidation, therefore increasing the oil film thickness on the cylinder wall. The increase of the oil film thickness increases the oil-scraping by the piston top land, and oil droplets detaching during the exhaust stroke. Jung et al. [43] reported that lubrication oil additives, such as calcium, can increase the oxidation rate of the lubrication oil, resulting in a decrease of the SOF mass.

CNG -fueled heavy-duty engines show similar characteristics [1, 7, 8, 9, 10, 11, 12, 13 and 14] have shown that the amount of elemental carbon in gaseous fueled engine exhaust is negligible compared to the organic carbon fraction. Ionic species and metals such as sulfates, phosphates, oxides of calcium, zinc, and magnesium are produced in the combustion chamber as a result of additives in the engine lubricating oil. These metallic compounds are added to the lubricating oil as detergents, dispersant, acid neutralizers, anti-oxidants, corrosion inhibitors, and anti-wear additives. In addition, wear metals from the engine can by carried into the combustion chamber by the lubricating oil. In a conventional diesel engine Essig et al. [44] found that a significant portion of the soluble organic fraction (SOF) in the exhaust PM came from the lubrication oil. In a typical engine exhaust PM the SOF is mostly made of poly-nuclear aromatics hydrocarbon (PAH), which has been associated with mutagenic and carcinogenic activity. Previous studies on the effect of PM emissions [36, 33] have concluded that the SOF can have harmful effects on human health.

Lubrication oil consumption has become an issue of major importance because of the tighter emission requirements imposed on modem engines. In gaseous-fueled engines, lubrication oil consumption assumes an important role, since it is one of the major sources of regulated emissions, excluding NO_x. Experiments have shown that gas-fueled engines have the same level of oil consumption as gasoline engines, operating under the same conditions [45]. Although Li et al. [46] found that in hydrogen engines oil consumption increases as the equivalence ratio increases, with an abrupt increase in oil consumption after knocking takes place.

The source of oil consumption in internal combustion can be divided into the following sources: piston-cylinder, valve train, crankcase ventilation system, and turbo charger. The most important is the piston-cylinder, which accounts for approximately 80 percent of the total oil consumption [47]. In addition the piston-cylinder accounts for 20 - 30 percent of the frictional losses in engines [48]. The dynamic process of oil consumption through the piston cylinder can be divided into the following components [49]:

1. Evaporation from the cylinder wall into the combustion chamber.
2. Oil throw-off by the top ring.
3. Reverse gas flow into the combustion chamber, carrying oil mist.
4. Oil scraping from the cylinder wall by the piston top land.

The oil evaporation from the cylinder wall becomes a very important oil consumption mechanism at very high engine loads, because the cylinder wall temperature increases, increasing the evaporation rate, and over time decreasing the oil viscosity [50]. Oil throw-off by the top ring occurs as a result of the inertia forces that act on the piston from the cyclic motion and oil accumulation on the top ring. Reverse gas flow into the combustion chamber is the result of a pressure difference between the combustion chamber and the piston second land [51]. During the compression stroke and the early parts of the expansion stroke the pressure in the top land is greater than in the second land, creating a gas flow toward the second land. The pressure in the second land builds up until the exhaust valve opens; afterward the pressure in the second land is greater than in the top land creating reverse gas flow. The oil scraping from the cylinder wall by the piston top land is created by the piston secondary movements [45].

In addition to the primary processes previously mentioned, studies found in literature refer to other conditions that can increase the oil consumption. Byung-Soon et al. found that oil

consumption is also affected by circumferential ring position; hence, ring rotational movement. Oil consumption was found to increase as the distance between the top and second ring gaps decreases. Furthermore they found that rings are more likely to move under no load conditions. Also under engine brake, no load, or light load conditions, the intake manifold pressure is lower than the crankcase pressure. The pressure difference causes oil to migrate to the combustion chamber where it is consumed [4, 39]. Engine knocking produces violent pressure waves that undermine the thermal boundary layer on the surface of the combustion chamber, exposing the surface to gases at very high temperatures. The increase in surface temperature increases the evaporation rate, which in turn increases the oil consumption [37]. Engine bore distortion is a condition that occurs at high speeds and high loads; causing ring separation that can substantially increase the amount of oil passing through the ring-liner interface, and gas blow-by [52].

This study proposes to characterize and determine toxicity as a function of volatility of ultrafine PM exhaust emission from CNG-fueled heavy-duty vehicle emissions. In collaboration with University of Southern California (USC), WVU proposes to conduct chassis dynamometer testing in order to achieve objectives stated above. We believe that the proposed test matrix comprising of transient, steady-state (40 mph) and idle modes of operation covers the range of a heavy-duty vehicle operation, which would affect oil consumption; hence, the mass and physical and chemical characteristics of PM emissions.

2.3 AMMONIA EMISSIONS FROM NATURAL GAS ENGINES WITH THREE-WAY CATALYST

The 2010 compliant natural gas engines have proven to produce a soot free exhaust. This fact helps these engines to meet the PM regulations without a particulate filter after-treatment system. However, in order to meet the current NO_x emissions limit of 0.20g/bhp-hr, manufacturers have adopted the stoichiometric combustion coupled with a three-way catalyst exhaust configuration. However, it has been widely documented that ammonia is a secondary pollutant formed during the NO_x reduction process over a three-way catalyst [53, 54]. Ammonia is usually formed due to the presence of both NO and H_2 in the exhaust stream. Two common mechanisms that result in the formation of ammonia on a three-way catalyst are [55]:

$$2NO + 5CO + 3H_2O \rightarrow 2NH_3 + 5CO_2 \qquad \textbf{(Eq. 2.1)}$$

$$2NO + 5H_2 \rightarrow 2NH_3 + 5H_2O \qquad \textbf{(Eq. 2.2)}$$

The dominant reaction for production of ammonia depends on the operating air/fuel ratio and the catalyst temperature. However, a significant amount of production of ammonia takes place during the presence of hydrogen molecules, which in turn is produced during periods of rich fuel/air mixtures [55]. In addition, contamination of the λ-sensor, used for dosing control, and cross sensitivity of the λ-sensor to other exhaust constituents may result in deterioration of NO_x conversion efficiency. Hydrogen could be either formed due to water gas shift reaction involving CO and water or the steam reforming reactions involving methane and water in the exhaust. However, the steam reforming reaction being an endothermic reaction requiring high temperatures would most likely occur during the combustion process [53]. The presence of high CO, unburned methane and high water content is well suited to the formation of ammonia in the exhaust of a three-way catalyst equipped stoichiometric natural gas engine.

2.4 AMMONIA EMISSION MEASUREMENT TECHNIQUES

Measurement of ammonia (NH_3) emissions from on-road vehicles has been found to a daunting task. Particular attention has to be paid to the sampling system to minimize measurement losses and possible sampling artifacts caused by the high reactivity and solubility of NH_3. Early tunnel studies in the 1980's [56] used impingers containing H_2SO_4 to capture gas-phase amines and ammonia, and Teflon membrane filters to remove solid-phase ammonium salts, alkylammonium salts and any amines adsorbed on aerosol particles. Subsequent ion- and gas-chromatography based methods were used to quantify NH_3 emission factors. Recent studies have employed Chemiluminescence (CLD or DCLD) methods [57, 58], Fourier-Transform Infrared Spectrometry (FTIR) [54, 58, 59, 60, 61], Non-Dispersive Ultra-Violet (NDUV) methods [62, 63, 64, 65 and 66], Tunable Diode-Laser Adsorption Spectrometry (TDLAS) [58, 67], different types of mass spectroscopy such as Chemical Ionization Mass Spectrometry (CIMS) [54, 60 and 61] and Soft Ionization Mass Spectrometry (SIMS) [58] as well as adsorption of gaseous NH3 in sulfuric acid with subsequent analysis by Ion Chromatography (IC) [54, 60 and 61].

Fitz et al. [57] compared CLD analyzers using simulated exhaust gas (artificially blended) with five different types of NO_2 to NO converters together with up to six different types of sample conditioning systems and heated sampling lines made of three different materials (Teflon, 316L stainless steel, 316L Silcosteel®). It was determined that NO and/or NO_2 were reacting with ammonia at elevated temperatures in the wet exhaust gas sampling stream; hence,

leading to NO_x losses in sampling lines and conditioning systems. It was further noticed that NO_2 to NO converters can oxidize NH_3 to NO depending on the converter age, water content in the sample stream and the converter matrix composition, causing a positive interference in NO_x readings. Nakatani et al. [58] developed a real-time NH_3 gas analyzer consisting of dual CLD detectors (DCLD) arranged in parallel where one of the CLD's was installed in series to a NH3 oxidation catalyst, which was housed in a furnace. Instantaneous NH3 values were calculated from the difference of the NOx readings. FTIR and SIMS measurements were performed with raw exhaust gas from a gasoline lean-burn vehicle using heated sample lines and compared to conventional sampling systems. Good correlations between NH3 results from all three measurement systems, namely DCLD, FTIR and SIMS, were found, with the DCLD having only minor differences in sharpness and maximum concentration of the signal peaks, which was attributed to the different sample gas handling conditions between the DCLD and FTIR/SIMS (the latter ones having longer sample lines). It was also noticed that the response time of the DCLD strongly depended on the material chosen for the gas filter with a T90 of approximately 7 sec for an optimized gas filter selection. Additional measurement comparisons were performed between the DCLD and a TDLAS system which was directly mounted to the tail-pipe using exhaust stream from a heavy-duty diesel engine equipped with a urea-SCR.

A comprehensive study to estimate the ammonia emission rates from 39 different light-duty vehicles (non-catalyst, Tier 0 to ULEV) over different chassis dynamometer test cycles was performed by Durbin et al. in 2002 [59]. Fourier-Transform Infrared Spectrometry (Pierburg AMA/Mattson system) was employed to measure NH3. The adsorption cell had a volume of 5 liters and a residence time for the sample gas of approximately 10 seconds. Diluted exhaust gas was sampled from the CVS tunnel (10" diameter, V_{mix} = 350 scfm) and directed through a ¼" heated line (110°C) with PTFE core to the FTIR. Additional heating pads were wrapped around the transfer tube, connecting the engine with the CVS tunnel to maintain exhaust gas temperatures above 120°C to minimize ammonia losses. However, it was reported that no difference in NH_3 readings between configurations with and without heating pads was observed. NH_3 measurements of replicate tests showed variability ranging from 10-20% for the majority of tested vehicles.

In 2004, Mohn et al. [60] made ammonia measurements on a EURO-I compliant gasoline vehicle, equipped with an OEM three-way-catalyst (TWC). One year later, Heeb et al. [54, 61]

conducted a follow-up to this study expanding it to NH_3 measurements on 12 additional EURO-III compliant gasoline passenger cars equipped with TWC's. NH_3 was detected using three different methods in parallel, namely Chemical Ionization Mass-Spectrometry (CI-MS, Airsense 2000, V&F GmbH, Austria), FTIR (Nicolet Avatar 370MCT, Thermo Nicolet Corp., USA) and Ion-Chromatography (DX-50, Dionex Corp. USA) from continuous NH_3 adsorption of a flow-proportional sample of raw exhaust gas in diluted sulfuric acid. For the FTIR measurement a heated, fully gold-plated Specac multipass-cell with a pathlength of 0.5m and an optical resolution of 4cm-1 was used. It was reported that all three measurement methods compared well with each other.

Exhaust gas was sampled, both raw, directly from the exhaust stack as well as diluted from the CVS tunnel to study possible sample interferences and measurement losses. Authors found NH_3 measurements from the CVS tunnel are subject to extensive reversible and irreversible adsorption/desorption, memory as well as surface reaction effects leading to severe sampling artifacts [54, 61]. Measurements showed that NH_3 was being absorbed by the CVS system during the initial part of a test cycle and subsequently released with a time delay. Results indicated ammonia release/desorption rate from the CVS system of the order of one hour; hence, affecting measurements of subsequent test cycles. It was assumed that the ammonia adsorption/desorption kinetics are mainly influenced by exhaust gas flow rate, surface-to-volume ratio in the CVS tunnel as well as the surface properties of the CVS tunnel such as the wall coverage with deposits or particulate matter [60]. The NH_3 adsorption effects were found to have a significant influence on the peak-shape of short-time emission events, namely the reduction in peak height, and therefore leading to a poor measurement resolution when measured diluted from the CVS tunnel [60]. Heeb et al. [61] mentioned that ammonia can be said to be chromatographically separated, due to its adsorption/desorption effects in the CVS tunnel, from species with lesser interaction activity with the CVS system. Furthermore, due to the high water solubility of NH_3 irreversible losses can occur which is especially pronounced in the wet sample stream of combustion generated exhaust gas. In order to minimize these effects water condensation should be avoided by means of heated sampling lines maintaining the sample stream temperature always above dew point temperature [61]. Also, possible condensation effects could occur in the tailpipe during cold start or when driving at lower ambient temperatures. Overall, it was found that irreversible losses, adsorption/desorption and memory

effects from diluted CVS measurements can lead to considerable over- (up to factor 4) or underestimation (up to factor 9) of ammonia in the exhaust gas [61]. It was concluded that the analysis of integrated samples of diluted exhaust (off-line), as well as the time-resolved monitoring of CVS exhaust gas at higher time resolution leads to wrong ammonia emission factors and therefore, NH_3 measurements from diluted CVS measurements or bag sampling methods should be avoided [54, 60 and 61].

Leippe et al. [65] tested a new Non-Dispersive Ultra-Violet (NDUV) measurement system (ABB, Limas 11-UV) for ammonia sampling that has been jointly developed by ABB and Volkswagen Germany [68] as an alternative to the established CLD method for the challenge of ultra-low NO_x measurements. The NDUV method has also been accepted by the US EPA for certification testing and details about calibration and interference checks can be found in 40 CFR, Subpart 86 and 1065. Leippe et al. [65] also discuss possible hang-up and diffusion effects of NO_2 and NH_3 within the sampling system due to their highly polar properties. It was concluded that NH_3 as well as NO_2 need to be measured raw and as close as possible to the emitting source. The highly water soluble properties of ammonia can lead to large portions being dissolved in condensed water which is especially pronounced for sampling methods that require the exhaust gas to be cooled down for water removal prior to the measurement system. It is therefore emphasized that in order to minimize hang-up effects and irreversible losses of NH_3 the exhaust gas sample stream within the lines and analyzer always needs to be maintained above dew point temperatures (150°-180°C). Further, it is mentioned that standard stainless steel is not an adequate material for sampling lines since NO_2 and especially NH_3 will react chemically with the surface at elevated temperatures. Possible alternatives are Silicosteels® which have a high molybdenum content, but they are rather expensive. A comprehensive study to evaluate possible sources of error and cross-sensitivity depending on the materials chosen for the sampling setup was conducted by Schiefer et al. [69]. It was found that sample lines made out of PTFE or similar fluor-chlorine-polymers exhibited favorable characteristics for exhaust gas measurements. Adsorption, diffusion and permeation effects between the sample gas and the polymer-lines are likely to occur. However, the adsorption rate for most of the gases was found to be negligible at temperatures below 190°C and a function of volume-to-surface ratio and residence time for temperatures above that. Leippe et al. [65] suggested using PTFE lines for ammonia sampling, and keeping them as short as possible to reduce adsorption and diffusion

effects since they may be more pronounced for NH_3 due to its very small molecules. To minimize these effects sample lines should be not much longer than 1m and lines for NH_3 calibration gas should not exceed about 3m.

Ciardelli et al. [66] compared the NDUV method (ABB, Limas 11HW) against conventional mass spectrometry to study SCR reaction kinetics in a microreactor setup. It was found that the NDUV system exhibited a fast response and was thereupon concluded that the system helped in improving the understanding of the catalytic SCR chemistry.

On-board measurements employing a Tunable Diode-Laser Adsorption Spectrometry (TDLAS) system were performed by Lenaers et al. [67] in 2006. The Norsk Electro Optik analyzer (Lasergas II, NH_3/H_2O monitor) with the transmitter and receiver mounted on the opposite sides of a compact measurement cuvet, allowed for on-line measurement of NH_3 in the full flow exhaust gas. The sampling path was heated to about 250°C to prevent loss of ammonia due to possible formation of ammonium nitrates (NH_4NO_3) and sulfates. It was reported that conventional IR analyzers usually require removal of water by use of a cooler which can lead to formation of NH_4OH (salts).

Recently (June 2010), the United Nations Economic Commission for Europe (UNECE) subgroup for transportation developed a draft for a possible ammonia measurement procedure [70] which is intended to serve as a proposal for future legislative texts. The basis for this proposal came from an existing outline of a test procedure for NH_3 measurement for the upcoming EURO-VI regulation for HD engines which is planned to contain a regulated ammonia limit over specified test cycles. The proposal points out that NH_3 sampling should be done raw, directly from the exhaust stack rather than from diluted CVS tunnel or sample bags due to the high reactivity and solubility of NH_3 with water. Sample lines should be made out of PTFE or special non-“sticky” stainless steel materials and should be maintained above dew point temperature and kept as short as possible. Two measurement methods are proposed so far, namely FTIR (by sample extraction) or TDLAS (in-situ), however, other systems or analyzers may be added to the final draft or may be approved by the approval authority, if they are found to yield equivalent results as the methods mentioned above. The proposal further specifies test procedures, data evaluation, analyzer calibration and specification as well as drift checks etc.

3 EXPERIMENTAL SETUP

3.1 VEHICLE EMISSIONS TESTING LABORATORY

The West Virginia University Transportable Heavy Duty Vehicle Emissions Laboratory consists of transportable heavy-duty chassis dynamometer and a transportable emissions measurement container.

3.1.1 Chassis Dynamometer

The chassis dynamometer test bed consists of rollers, flywheel assembly, eddy current power absorbers, differentials, hub adapter, torque and speed transducer built onto a tandem axle semi trailer (see Figure 2 and Figure 3). The hydraulic jack on the chassis dynamometer test bed is functional in setting the test bed on the ground and onto the trailer. The various components of the chassis dynamometer are discussed in detail below.

Rollers: The chassis dynamometer consists of a set of two paired rollers in the front which supports the single or forward drive axle and a set of single roller at the back in order to support the rear axle of tandem axle vehicles. The rear pair of rollers can be placed in three different positions to accommodate tandem spacing of 4 to 5 ft (1.22 – 1.52m) and each roller is 12.6 inch (32 cm) in diameter with their axis along the length of the test bed. Each pair of rollers is linked by a flexible coupling to have uniform rotational speed on either side of the vehicle and the coupling was designed to accept 20% of the wheel torque in case of any imbalance due to uneven surface at the test location.

- Hub Adapters: The hub adapters are used to couple the engine drive axle with the flywheel assembly and eddy current power absorber via torque and speed transducer. The adapter is made of a 0.5 inch (13 mm) thick aluminum plate of diameter 1.8 ft (0.55 m).
- Load Simulation System: The load simulation system consists of a flywheel assembly, an eddy current power absorber, a speed and torque transducer, double differentials and universal couplings on either side of the vehicle to be tested as shown in the figure below. The power from the vehicle's drive axle is transmitted to the flywheel assembly and power absorbers by a hub adapter which is connected to a 24 inch (61 mm) long spline shaft running into a pillow block. The spline shaft is connected to the speed and torque transducer by a universal coupling which can withstand torque up to 16,415 lb-ft (222,256 N-m) on either side. The speed and torque transducer is capable of providing the data logging computer with time varying output torque at a rate of 10 Hz. The torque transducer drives a

second shaft via companion flange. This shaft transfers power to a right-angle speed increasing drive, a double reduction differential with a ratio of 1:3.65 which drives the flywheel assembly and a second differential. The second differential with a ratio of 1:5.73 drives the eddy current power absorbers.

- Flywheel Assembly: The flywheel assembly is designed to simulate vehicle gross weights of 40,000 to 66,000 lb. With the maximum being 40,000 lb (18,144 kg) at a wheel diameter of 4 ft (1.22 m) and 66,000 lb (30,000 kg) at a wheel diameter of 3.25 ft (1 m). The flywheel assembly consists of a drive shaft with four drive rotors running in two pillow blocks. Each drive shaft supports eight flywheels of different sizes with bearings resting on the shaft. By selectively engaging the flywheels to the drive rotors, vehicle mass can be simulated in 250 lb (113 kg) increments.
- Eddy Current Power Absorbers: A Mustang model CC300 air cooled eddy current dynamometer mounted on two bearings is used as power absorbers. The power absorbers are used to simulate load due to rolling friction of the tires and the aerodynamic drag resistance. The eddy current dynamometer has the capability of absorbing 300 hp (224 kW) continuously and 1000 hp (745.7 kW) intermittently during peak operation. Dynamometer load at any speed is controlled by the direct current supplied to the coils and the power absorbed is measured by the torque arm force transducer (load cell).

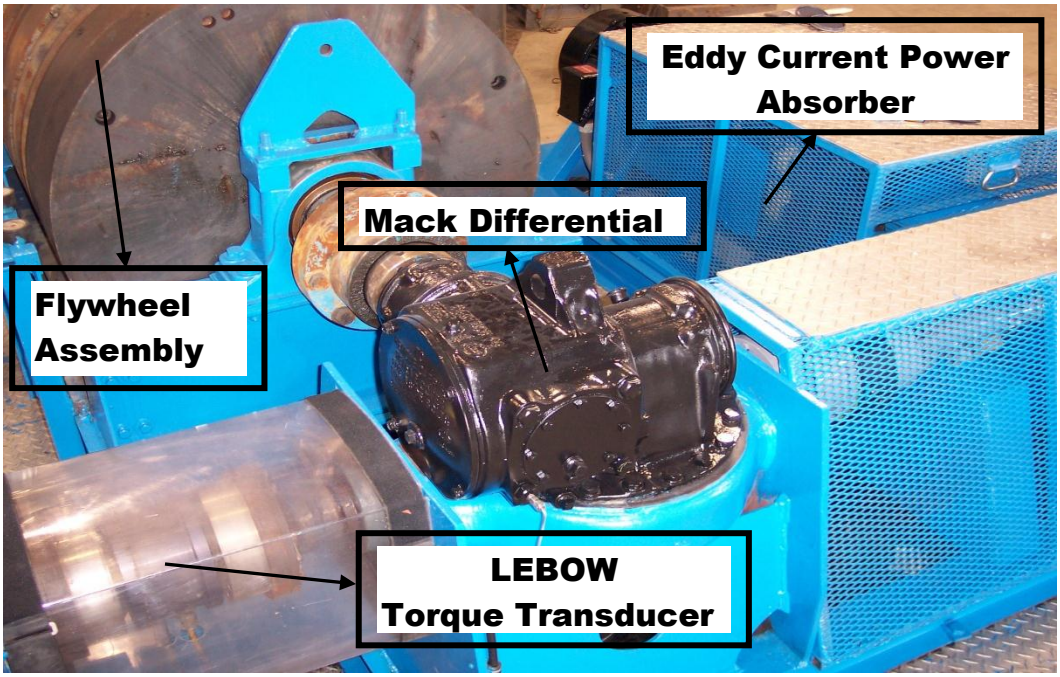

Figure 2 Components of a Chassis Dynamometer

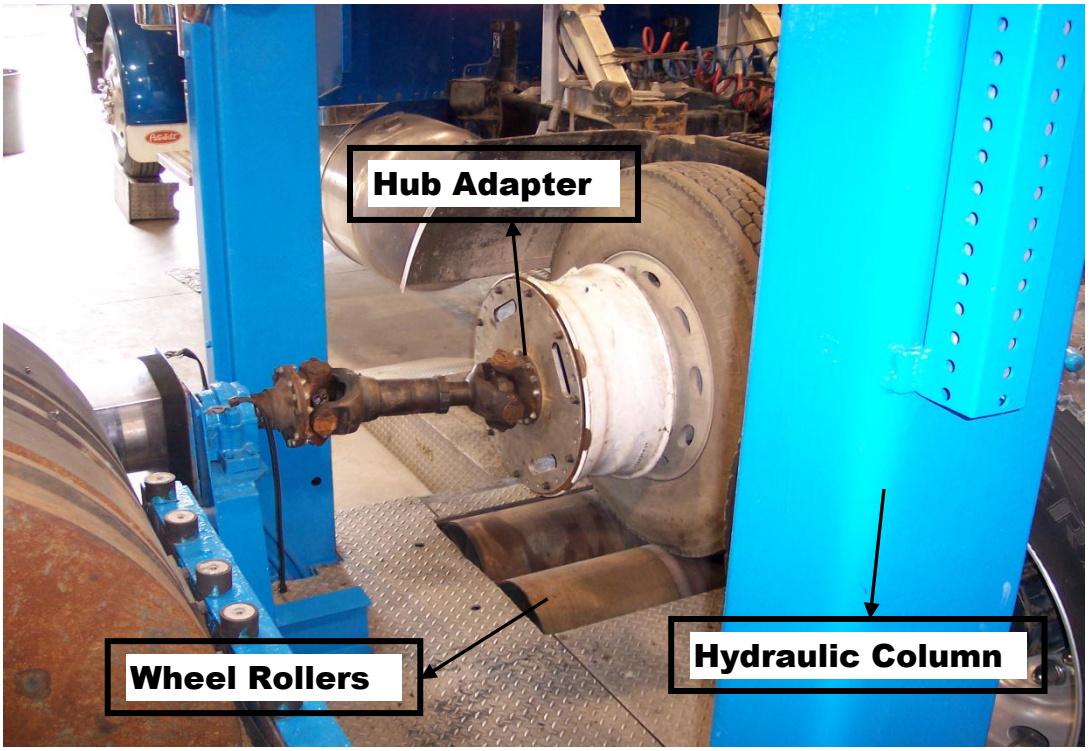

Figure 3 Connecting and supporting structure of chassis dynamometer

While the driver is responsible for the control of the speed, the transient torque must be controlled by an automated system. The load supplied by the flywheels simulates the static weight on the engine and is controlled by their rotational speed, while the load due to rolling friction and wind drag is simulated by the eddy current dynamometer. The eddy current dynamometer is controlled by a Dyn-Loc IV control system provided by Dyne-Systems. The Dyn-Loc IV control system operated by a PID control loop where "P" stands for proportional control in which the controller calculates error between the actual and the desired output resulting in a restoration signal linearly proportional to the error. "I" stands for integral control in which the controller calculates the average error over a time and provides a restoring signal which is the product of the error and the time the error persisted. It is used to restore the original set point. D stands for differential control in which the controller calculates the rate at which the set point is changed and produces a corrective signal to reach the set point quickly. Hence, PID controller provides a fast and smooth response in controlling the transient set points. During the test, the power absorbers receive the torque set point from the dyne-loc controller. The set point is equal to the road load power and it is calculated using the following equation (Eq. 3.1):

$$P_r = (C_r Mg + \frac{1}{2}\rho_a C_D A V^2)V \qquad \textbf{(Eq. 3.1)}$$

Where:

P_r = Road load power

C_r = Coefficient of rolling resistance

M = Vehicle gravitational mass

ρ_a = Air density

A = Frontal area of vehicle

C_D = Coefficient of drag

V = Vehicle speed

The set point is updated every 100 milliseconds. The speed and torque values are logged at a frequency of 10 Hz to ensure the test has been performed to the specification.

3.1.2 Emissions Measurement Container

The housing for the new transportable laboratory is a reconstructed 9.1m (thirty-foot) long cargo container which houses a HEPA primary dilution unit, two primary full-flow dilution tunnels, a subsonic venturi, a secondary particulate matter sampling system, a gaseous emissions analytical bench instrumentation system, a computer-based DAQ and control system, a heating, ventilating and air conditioning (HVAC) system, and chassis dynamometer control systems. Figure 4 shows the schematic of the transportable laboratory container. The two primary dilution tunnels inside the container, of 0.46 m (18 inches) ID and 6.1 m (20 feet) long, were designed to provide dedicated measurement capability for both low PM emissions ("clean") vehicles (with the upper tunnel referred as the "clean tunnel"), as well as traditional diesel-fueled vehicles with high PM levels (lower tunnel referred as "dirty tunnel"). This provision reduces tunnel history effects between test programs of differing exhaust emission composition. A stainless steel plenum box houses two HEPA filters for filtering primary dilution air, as well as twin dual-wall exhaust transfer inlet tubes dedicated as exhaust inlets for the upper and lower tunnels. The HEPA plenum is connected into the main dilution tunnels, which are selectively connected to the subsonic venturi via stainless elbow sections. The air compressor and two vacuum pumps are installed inside a noise isolating overhead. An air tank stores compressed air and provides shop air to the zero air generator (a device removes PM and THC) for instrumentation use. A PM sampling box for the secondary dilution tunnels is located alongside the primary tunnels, downstream of tunnels' sample zones. The secondary PM dilution tunnel of either the dirty or

clean tunnel is connected to the PM sampling box for PM measurement during the test. Figure 5 shows the transportable laboratory container on the transportation Landoll 435 trailer.

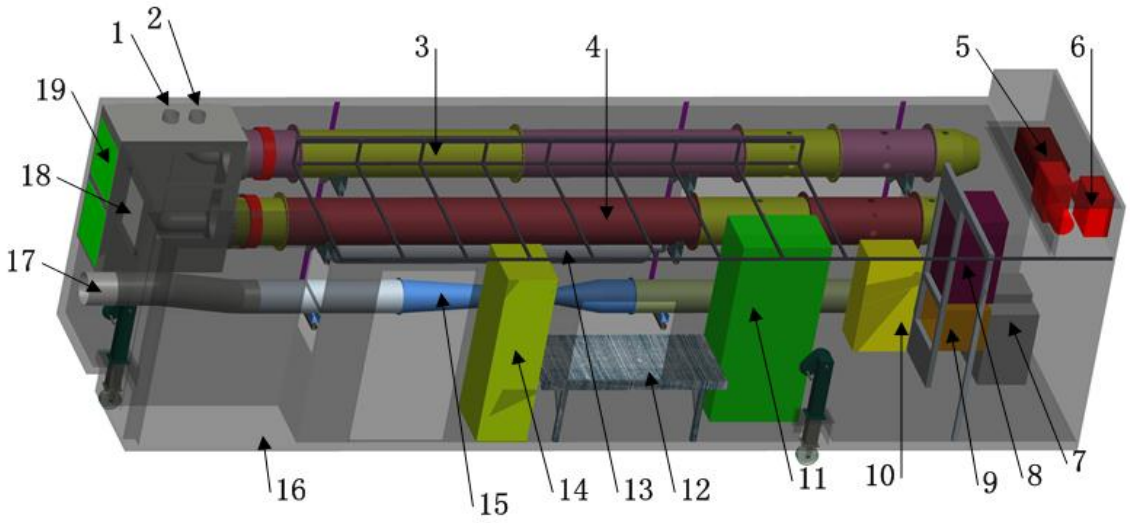

Figure 4 Schematic of the transportable laboratory container

1- Exhaust inlet of dirty tunnel; 2- Exhaust inlet of clean tunnel; 3- Clean tunnel; 4- Dirty tunnel; 5- Air compressor; 6- Vacuum pumps; 7- Oven; 8- PM sampling box; 9- Glove box; 10- Zero air generator; 11- MEXA-7200D motor exhaust gas analyzer; 12- Computer table; 13- Air tank; 14- DAQ rack; 15- Subsonic venturi; 16- Air conditioner deck; 17- Outlet to blower; 18- Ventilation fan; 19- HEPA filters

Figure 5 View of the transportable laboratory container

3.1.2.1 Gaseous Emissions Sampling System

The gaseous emissions measurement system was designed to be capable of measuring raw exhaust and diluted emission levels. Emissions levels vary continuously over transient test cycles. Final emissions values must be determined with correction for background level. The background sample flow is taken from a sample probe located immediately after the HEPA filters inside the plenum box. A diluted sample flow is also drawn from the sample probe installed at the primary sample zone, providing a bag of composite diluted exhaust, which is analyzed along with the background bag. While the purpose of the background batch sampling is to correct for background gaseous emission levels, the diluted batch sampling provides for a check on integrated continuous values for quality control purposes. In some cases, where the emissions vary over a wide concentration range over a cycle, a dilute bag analysis may also provide a more accurate assessment of those species than can be obtained by integration. This is often the case for CO from legacy diesel vehicles over severe transient cycles.

The container is equipped with Horiba MEXA 7200D motor exhaust gas analyzer for gaseous measurements from the dilution tunnel. The MEXA7200D is capable of measuring all regulated emission species that include THC, CO, CO_2, NO_x and methane through a non-methane cutter equipped secondary hydrocarbon channel. The unit can be fitted with various analyzer modules, and the current configuration consists of AIA-721A CO analyzer, an AIA-722 CO/ CO_2 analyzer and a CLA-720 “cold” NO_x analyzer part of the cold sample stream and the FIA-725A THC analyzer and CLA-720MA NO_x analyzer part of the heated sample stream.

3.1.2.2 PM Sampling and Measurement System

The measurement container houses the PM sampling system for the transportable laboratory. However, the measurement system of pre-weighing and post weighing the gravimetric filters are carried out in Morgantown, WV at the WVU facility which houses a class 1000 clean room, with controlled environment for accurate weighing of the filters. The measurement system is operated with in-house developed software to calibrate the scales, perform measurements, and also to monitor the filters history. The schematic of the on-board PM sampling system is as shown in Figure 6.

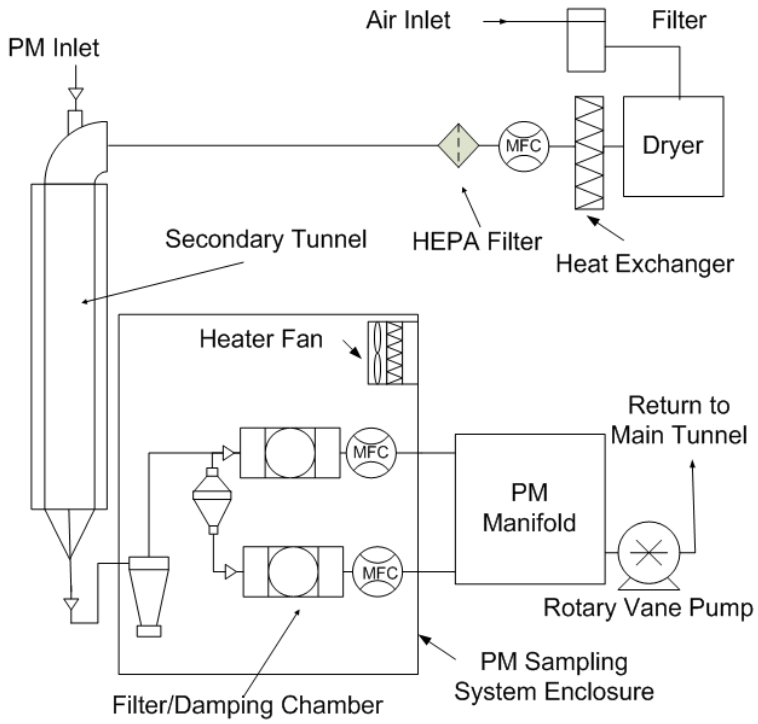

Figure 6 Schematic of the PM sampling system

Figure 7 shows the view of the temperature controlled PM sampling system with two independent streams for the clean tunnel and the dirty tunnel.

Figure 7 1065 compliant PM sampling system on-board the transportable laboratory container

The sampling system consists of the dilution air stream, which is filtered and cooled to remove moisture. The dry dilution air is then heated to 25±5°C as per regulations prescribed in CFR 1065. The conditioned secondary dilution flow is subsequently introduced to the main PM flow drawn from the primary dilution tunnel and allowed to mix in the secondary dilution tunnel. The size of the secondary dilution tunnel was determined by Simulink modeling [71]. The secondary tunnel wall is maintained at 47°C. The flow from the secondary tunnel enters in to the PM sampling chamber through a $PM_{2.5}$ cyclone and into the 47mm filter holder. The PM system consists of two streams with two separate cyclones and filter holders, connected to the two different primary dilution tunnels. The PM box is also maintained at 47°C. All flows are controlled by calibrated mass flow controllers.

3.1.2.3 CVS Flow Control

The laboratories CVS flow control is achieved through a sub-sonic venturi (SSV). The SSV installed on the transportable laboratory was supplied with 300 series Schedule 5 stainless steel pipe sections, with a nominal internal diameter of 12" The SSV throat diameter was 6.26". To ensure the accuracy and repeatability of SSV flow rate measurement, a straight section of Schedule 5 pipe, ten feet in length, was flanged and attached to each end of the subsonic venturi to minimize the flow wakes, or eddies, or flow circulation which might be induced by pipe bends or coarse inside walls. This particular SSV was calibrated with a reference SSV from 400 scfm to 4000 scfm following the procedure defined in 40 CFR Part 1065.340. The flow rate of the SSV is calculated, in real time, using the equations in 40 CFR Part 1065.640 and 40 CFR Part 1065.642.

3.2 TEST VEHICLE AND ENGINE SPECIFICATIONS

Two transit buses from the Sacramento transit agency were used for the study. The buses were CNG fueled and initially intended to be of one high mileage and one lower mileage test vehicles. However, the since the buses were all commissioned relatively at the same point into the fleet, the mileage differences were not significant. Hence, the test plan was modified to procure and test two buses with similar odometer readings. Table 1 and Table 2 list the vehicle and power train specifications of the Sacramento transit buses tested in this study.

Table 1 Test vehicle specifications

Bus #	Vehicle ID	Chassis Manufacturer	GVWR	Odometer Reading	Vehicle Model Year	After-treatment System	Fuel
2834	1VHGH3W2586703737	Daimler Bus North America	42540	77538	2008	3-Way Catalyst, Cummins	CNG
2824	1VHGH3W2486703602	Daimler Bus North America	42540	84994	2008	3-Way Catalyst, Cummins	CNG

Table 2 Test vehicle power train specifications

Engine Manufacturer	Engine Model	Engine Model Year	Displacement/Power (L/HP)	Type of Fuelling	NOx/PM (gm/bhp-hr) *
Cummins	ISLG 280	2007	8.9 / 280	CNG Stoichiometric	0.2 / 0.01

** Values indicate the USEPA emissions standard compliance of the engine*

3.3 TEST CYCLE

Three test cycles were used for this study. Urban Dynamometer Driving Schedule (UDDS), 45 MPH steady state and idle test.

The UDDS cycle simulates the freeway and non-freeway operation of a heavy-duty vehicle. The UDDS was also use as the basis to develop the Federal Test Procedure (FTP) engine dynamometer cycle. The cycle is of 1060 seconds in duration with a maximum speed of 58 MPH. The vehicle is exercised over 5.5 miles over the entire test cycle. Due to the expected low PM emissions levels from the test vehicles triplicate versions of the UDDS driving cycles were created. Regulated emissions were calculated over a triplicate length UDDS cycle and unregulated media were sampled over three repeats of a triple length UDDS on one media.

The 45 MPH steady state cruise cycle was created for an hour long. Idle test point was sampled for 1 hour length of idle and emissions reported as grams/sec of idle. Figure 8 shows the 16.5 mile long and 53 minute duration triple-UDDS cycle.

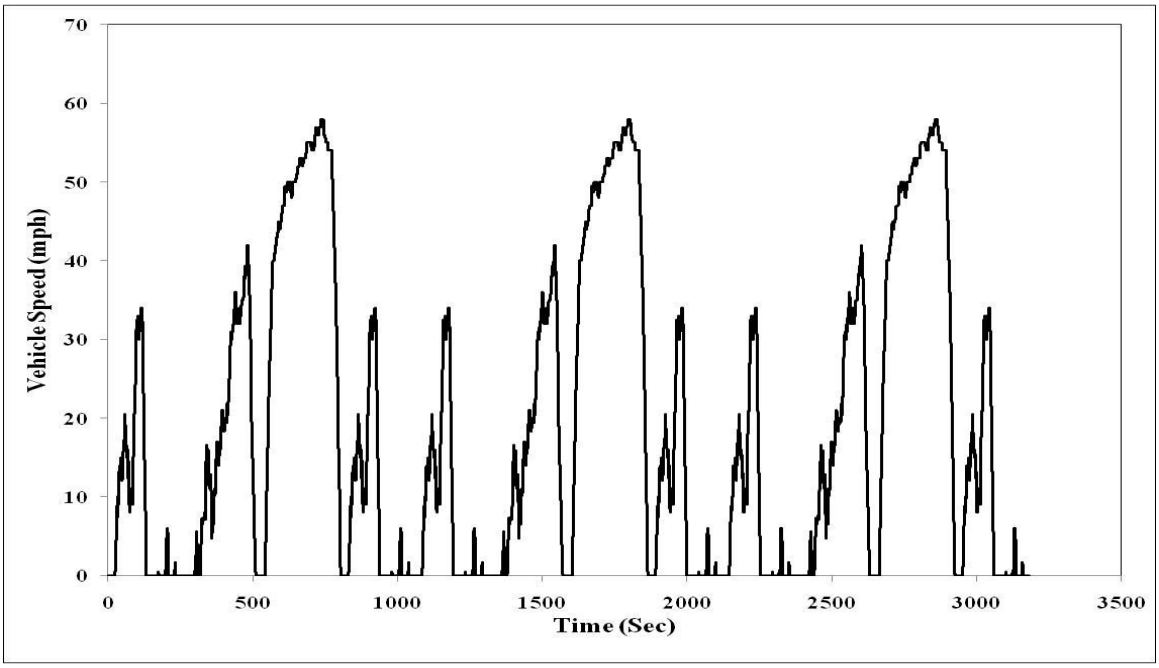

Figure 8 Speed vs. Time trace of triple-UDDS cycle

3.4 THERMODENUDER PM SAMPLING SYSTEM

Thermodenuder PM sampling system was designed and built at WVU to perform high volume sampling of thermally denuded and non-denuded PM samples on filter media. The system was designed to contain 4 thermal denuders, with independent flow control using mass flow controllers. Samples downstream of the denuders were collected onto separate 47mm T60A20 filters. The sampling system also housed the temperature controllers for the denuders. The sampling system also contained the 5^{th} sampling stream for the non-denuded sample collection. This stream was designed as a high volume sampling stream with flow rate of 200lpm, controlled by a calibrated critical flow orifice. Thermal denuders were air cooled by circulating compressed air through its cooling stream. Figure 9 and Figure 10 show the thermodenuder sampling system setup.

Figure 9 Outside view of thermodenuder sampling system.

Figure 10 Inside view of thermodenuder sampling system

National instruments DAQ NI-USB6009 was used to record flow, temperature, pressure and also to control the set points of the mass flow controllers. National Instruments Lab View software was used to create the data acquisition program for the sampling system. The system

initiation was linked to the container in order to sync data collection with the main container DAQ system.

3.5 AMMONIA MEASUREMENT SYSTEM

Although ammonia measurements were not part of the work plan, certain observation during the course of the testing prompted WVU to install an ammonia measurement system. Due to the difficulties associated with ammonia measurement from the CVS tunnel as discussed in previous sections a raw ammonia measurement technique was adopted. Heated stainless steel sampling lines, heated pumps and heated filters were employed to transfer raw exhaust into the analyzer. The temperature set point for the heated sampling system was maintained at 375°F. The Ecophysics CLD 844 CM-hr analyzer was used for quantification of ammonia. The analyzer works on the principle of chemilumniscence for detection of NO_x. The analyzer employs two channels, one to detect total NO_x and the other to NO_x-amines. The NO_x-amine stream consists of a catalyst that converts all ammonia in the sample stream to NO_x-amines. And as a result the difference in the two channels would result in the ammonia concentrations. The analyzer consists of heated inlets to prevent water and ammonia condensation within the system.

3.6 PARTICULATE MATTER SIZING SETUP

The study employed the Engine Exhaust Particle Sizer Spectrometer (TSI EEPS Model 3090) for transient particle size distribution measurement and the Electrical Aerosol Detector (TSI Model 3070A) to monitor the instantaneous particle concentration with respect to an aerosol parameter called total aerosol length. Both the EEPS and the EAD were setup up for sampling from the CVS dilution tunnel. This method of sampling was chosen over partial flow dilution of raw exhaust using ejector pumps in order to better correlate the gravimetric PM and the particle size distribution and concentration formed as a result of dilution within the CVS. Further the PM size distribution and concentration data could also be associated with toxicity data as dilution conditions for both sampling stream are the same. As preliminary procedures sample flow rates of the EEPS were verified with a standard flow meter, and the operation of the instrument was checked against the standard TSI SMPS 3936. The instrument was cleaned and electrometers were zeroed before the commencement of the study.

Since the EEPS was sampling directly from the CVS tunnel, the only applicable dilution ratio is based on the exhaust flow ($V_{exhaust}$) and the total CVS flow (V_{mix}); hence, is a function of engine operation.

$$DR = \frac{\dot{V}_{mix}}{\dot{V}_{exhaust}} = \frac{[mol/s]}{[mol/s]} = [-] \qquad \textbf{(Eq. 3.2)}$$

Due to the lack of accurate exhaust flow measurements, the dilution ratio has been approximated based on a simplified carbon balance, assuming stoichiometric combustion (Eq. 3.3), methane (CH_4) and ideal air (21% O_2, 79% N_2) as the sole reactants as well as no carbon content (CO_2, CO, HC) within the dilution air, and the continuous measurement of CO_2 within the CVS tunnel. According to Equation 3.3 for each mole of CO_2 produced one mole of CH_4 is being consumed. Therefore, multiplying the amount of CO_2 measured at the CVS sample plane with the total flow through the CVS system (V_{mix}) gives the molar rate of CH_4 burned as shown in Equation 3.4.

$$CH_4 + 2(O_2 + 3.76N_2) \rightarrow CO2 + 2H_2O + 7.52N_2 \qquad \textbf{(Eq. 3.3)}$$

$$CH_4[mol/s] = \frac{CO_2[ppm]}{10^6} \cdot \dot{V}_{mix} \qquad \textbf{(Eq. 3.4)}$$

Further, using the theoretical air-fuel ratio (AFR_{molar}) on a molar basis (9.52 for CH_4), calculated from the stoichiometric reaction equation (Eq. 3.3) the molar rate of intake air flow and exhaust flow can be estimated based on (Eq. 3.5) and (Eq. 3.6), respectively.

$$\dot{V}_{Intake}[mol/s] = CH_4[mol/s] \cdot AFR_{molar} \qquad \textbf{(Eq. 3.5)}$$

$$\dot{V}_{exhaust}[mol/s] = \dot{V}_{Intake}[mol/s] + CH_4[mol/s] \qquad \textbf{(Eq. 3.6)}$$

3.7 UNREGULATED EMISSIONS SAMPLING SYSTEM

The samples of unregulated emissions were drawn at the second sampling section downstream of the regulated emissions sampling section. The unregulated emissions sampling system consisted of various sampling trains to sample different emissions which are described in the following sections.

3.7.1 Carbonyls

The carbonyl sampling system consisted of a heated probe and a heated sampling line whose temperatures were maintained at 240^{o}F (115.5^{o}C) to prevent water condensation. A flow of 2 lpm was maintained using a calibrated critical flow orifice and a vacuum pump. The sample was collected into cartridges packed with silica gel coated with acidified 2, 4-dinitrophenylhydrazine (DNPH). The cartridges were then shipped to a CARB MLD laboratory for subsequent analysis.

3.7.2 Polycyclic Aromatic Hydrocarbon (PAH/n-PAH) Sampling System

Polycyclic Aromatic Hydrocarbon was sampled from the tunnel into PUF/XAD cartridges. Sample from dilution tunnel was drawn at 200 lpm. The flow control was achieved through a critical flow orifice. The sample is admitted into the sampler through a copper tube and into a manifold which contains the housing for the PUF/XAD cartridge. Figure 11 shows the schematic of the PUF/XAD cartridge housing. The housing holds the PUF/XAD cartridge and a 70mm T60A20 filter used to capture the PM bound organic compounds. The pumps are initiated manually with the start of the test.

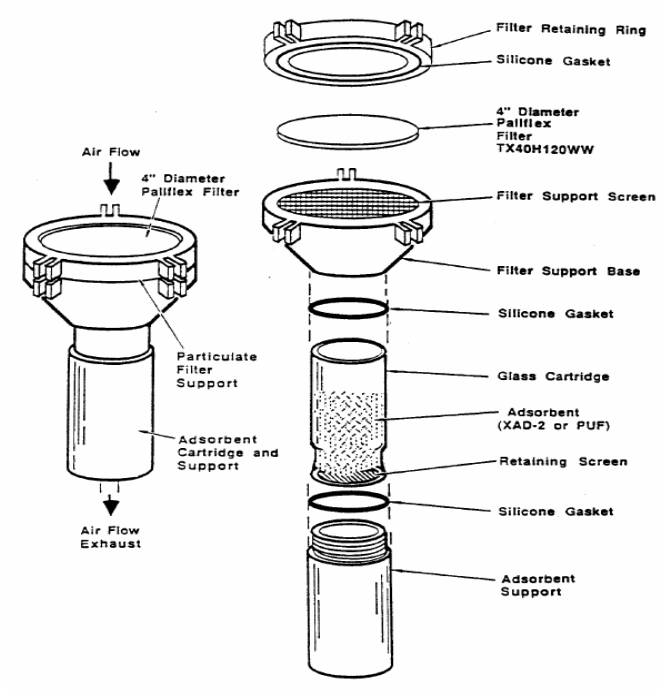

Figure 11 Schematic of DRI's PUF/XAD cartridge housing

3.7.3 VOC Canister Sampling System

VOCs were collected into a steel canister for laboratory analysis using a critical flow orifice system provided by CARB Monitoring Laboratory Division. The canister had a capacity of 6.0L at atmospheric condition. The steel canisters used to collect dilute exhaust were completely evacuated, and a vacuum of 10mm Hg was present inside the canister prior to the start of the test. Sample was collected below atmospheric pressure to prevent water condensation. The vacuum inside the canister was used to draw the sample from the tunnel, through the critical flow orifice.

3.7.4 Cyclonic Particle Classifier

Sampling of unregulated emissions included gravimetric analysis of particulate matter in size fractions of 10μm, 2.5μm and 1μm. This was accomplished by using cyclonic classifiers. Cyclone classifier makes use of vertical flow inside a cylindrical or conical chamber to separate particles depending on the flow rate. A double vortex flow is induced in the conical body of the cyclone by introducing the sample tangentially at the top where flow spirals down along the wall, which then reverses and spirals through inner core to exit the chamber. Particles with sufficient inertia impact on the cyclone wall as they cannot follow the streamlines of the flow exiting the chamber. The various size fractions of PM were sampled directly from the primary dilution, as the tunnel was built to a single stage PM sampling specification. The samples were collected on a 47mm Teflon coated glass fiber filters (T60A20). The flow through the cyclone was controlled using mass flow controllers.

3.7.5 Gas Bag Sampling

Tedlar bags were used to collect samples of dilute exhaust gas and dilution air during each emissions test. The bag samples were analyzed to find the integrated concentrations and the contribution of dilution air to the actual emissions. The dilute exhaust bag served as a QA/QC check point when compared with the continuous sample.

3.8 INSTRUMENTATION CONTROL AND DATA ACQUISITION

A software application developed in-house controlled the power absorbers and the data acquisition system. The program acquired the raw data (ADC codes) and a reduction program converted the raw data into proper engineering units using respective calibration curves.

3.9 MEDIA

Different types of media were used to collect samples for speciation and gravimetric analysis during the test procedure. The media were conditioned, weighed and handled as per the regulations outlined in CFR, Title 40. A list of species and the media used to collect them is given in the Table 3.

Table 3 List of species and sample media

Species	Collecting Media
Volatile Organic Compound (VOC),	VOC Steel Canister
PAH, n-PAH	TX 40 70 mm Filter + PUF/XAD Cartridge
Aldehydes	DNPH Cartridge
PM2.5 Metals/Ions	Teflo (47mm) Filter
PM1.0/PM 2.5 Gravimetric	T60A20 (47mm) Filter

3.10 MEDIA CONDITIONING AND WEIGHING

The media used in collecting PM for gravimetric analysis were conditioned and pre-weighed in the WVU EERL facility before transporting them to the test site. The filters were conditioned in an environmentally controlled chamber (Class 1000) maintained at 70^{o}F with a relative humidity of 50%, for at least 1 hour and not more than 80 hours before being weighed according to 40 CFR, Part 1065 specifications. The 70mm filters were placed in the glass petri dishes and 47mm filters were placed in plastic analyslides, with their lids closed but not sealed in order to prevent dust from accumulating on the media while allowing for humidity exchange. Two reference filters were conditioned with the test filters and placed in the environmental chamber in order to account for change in the filter weight due to fluctuation in humidity. The reference filters were weighed before and after any set of media were weighed to ensure that the conditions in the environmental chamber were stable.

The filters were pre-weighed after a stabilization period of 24 hours using a Metler - Toledo Microbalance. The balance was interfaced with a computer in which the filter weights were logged for future reference and use. The filters were conditioned for several hours in the chamber before the petri-dishes were sealed and packed in padded envelopes for shipping to the test site.

3.11 MEDIA SHIPPING AND TRACKING

The petri-dishes containing the filter media were sealed and placed in padded envelopes after they had been pre-weighed. The set of envelopes containing media required for one test were placed together to aid in quick loading of the media into the sampling system. The sealed media were transported overnight to the test site in coolers filled with frozen water pouches. After the media was received at the test site it was placed in the conditioning room until used. A media tracking application was developed to identify the media with the test sequence and run number. The tracking tool also aided in QA/QC protocol. The used media were placed back into their respective petri-dishes in the conditioning room and were tracked before shipping to the location, where they were analyzed.

4 EMISSIONS TESTING PROCEDURE

4.1 SET-UP

The chassis dynamometer which is built onto a flat bed trailer was set-up on a flat surface and leveled to prevent variation in the vehicle's inertial loading which is simulated using rotating flywheels. The emissions measurement container which houses the analyzers, dilution tunnel, dynamometer control and signal conditioning devices was placed close to the chassis dynamometer. This reduced the length of exhaust tubing between the tail pipe and the dilution tunnel in turn reducing thermophoretic and other losses of particulate matter in the transfer tube. The blower was placed at the end of the dilution tunnel and a flexible air duct was used in connecting the tunnel to the blower. HEPA filters were installed to the inlet manifold of the dilution tunnel. After all the connections were made to the dilution tunnel the instrument trailer was prepared for testing.

4.2 LABORATORY CHECKS

Initial laboratory set-up procedures include complete measurement system verification followed by calibration. All required system verifications are performed as per requirements stated in 40 CFR, Part 1065, Subpart D. The measurement container is equipped with the Horiba Mexa 7200 Motor Exhaust Gas Analyzer, which is capable of automatically performing the required analyzer verification tests. The verification procedure and pass criteria of the tests were in accordance to the provisions described in 40 CFR, Part 1065, Subpart D. Table 5 lists the complete set of analyzer verification checks performed on field prior to the commencement of the testing. Table 4 lists the complete set of leak checks performed on the gaseous and PM measurement systems.

Table 4 Gaseous and PM measurement system verification checks

Leak Checks	Pass Criteria
Leak and Delay Time Check (all analyzers)	Within ± 5% over 30 sec interval
PM System 1 Leak Check	
PM System 2 Leak Check	

Table 5 Analyzer verification checks

Analyzer Checks	Pass Criteria
THC1 Hang-up	
THC2 Hang-up	
CO(L), CO_2 Interference Check	Within ±1%
THC, O_2 Interference Check	Within ± 2%
CO_2 Quench NO_x1	Within ±1%
CO_2 Quench NO_x2	Within ±1%
H_2O Quench NO_x1	Within ±1%
H_2O Quench NO_x2	Within ±1%
Non-Methane Cutter Efficiency	$PFCH_4$>0.85 and PFC_2H_6<0.02

4.3 MASS FLOW CONTROLLER CALIBRATION

Mass flow controllers were used in controlling the flow through cyclonic particle classifier, TPM flow through the filter and various other unregulated emissions sampling systems. The calibration was performed against a Laminar Flow Element supplied by Meriam Flow Measurement Devices. Meriam provides a calibration equation and co-efficient for each LFE which is obtained through calibration involving a flow meter that is traceable to NIST standards. A five point calibration was performed on the MFCs between fully open and fully closed position. The flow through the LFE was calculated using the following equation:

$$Vactual = \left[B \cdot (\Delta P) + C \cdot (\Delta P)^2\right] \cdot \left(\frac{\mu_{std}}{\mu_{flow}}\right) \qquad \textbf{(Eq. 3.7)}$$

Where

B & C = LFE specific co-efficient

ΔP = Pressure differential measured across LFE

$\frac{\mu_{std}}{\mu_{flow}}$ = Viscosity correction factor

The viscosity variations were calculated using the correction factor given in the following equations:

$$CorrectionFactor = \left(\frac{529.67}{459.67 + T(°F)}\right) \cdot \left(\frac{181.87}{\mu_g}\right) \quad \textbf{(Eq. 3.8)}$$

$$\mu_g = \frac{14.58 + \left(\frac{459.67 + T(°F)}{1.8}\right)}{110.4 + \left(\frac{459.67 + T(°F)}{1.8}\right)} \quad \textbf{(Eq. 3.9)}$$

Differential pressure across the LFE and absolute pressure was measured using a Heise pressure reader and the temperature was measured using a Fluke Temperature calibrator. The actual flow measured through the LFE was converted to standard flow by 40 CFR, Part 1065 specified standard condition of 20^{o}C and 101.1kPa.

4.4 CVS-SSV DILUTION TUNNEL VERIFICATION

The CVS system was verified by injecting a known quantity of propane into the primary dilution tunnel while CVS-SSV system operating. The concentration of the propane was determined using a pre-calibrated HFID analyzer and the mass of propane injected was measured by the flow data and the density of propane. The propane injection test helped in determining leak in the tunnel and any discrepancy in the flow measuring device (CVS-SSV system).

The method uses a propane injection kit with a critical flow orifice meter to accurately measure the amount of propane injected into the tunnel. The flow rate of propane through the orifice meter is determined by measuring the inlet temperature and pressure using the following equation:

$$q = \frac{A + (B \cdot P) + (C \cdot P^2)}{\sqrt{460 + T(°F)}} \quad \textbf{(Eq. 3.10)}$$

Where:

q = Flow rate through orifice in scfm at standard condition (20^{o}C and 101.1kPa)

A, B, C = Calibration coefficients provided by the orifice manufacturer

P = Absolute orifice inlet pressure, in psia (guage + atmospheric pressure)

T = Orifice inlet temperature in ^{o}F

The total flow through CVS is given by the following equation:

$$Q = \frac{\dot{V}}{t} \cdot 60 \qquad \textbf{(Eq. 3.11)}$$

Where:

Q = Total volume in scf

V = Flow rate in scfm measured by CVS

T = Time interval in seconds, usually 300 seconds

The calculated sample concentration was determined by the following equation:

$$C_{calc} = \left(\frac{q}{Q} \cdot 10^6 \right) \cdot 3 \qquad \textbf{(Eq. 3.12)}$$

The system error was then given by:

$$Error = \left(\frac{C_{obs}}{C_{calc}} - 1 \right) \cdot 100 \qquad \textbf{(Eq. 3.13)}$$

Where:

C_{obs} = Measured concentration of the injected propane by HFID analyzer

If the error is greater than $\pm$ 2%, then the cause for discrepancy was found and corrected. The error could be due to various reasons such as leaks before the sampling plane, leaks after the sampling plane and improper analyzer calibration. Three repeatable propane injections within a difference 0.5% of each other is required to pass the dilution tunnel verification test.

4.5 TEST PROCEDURE

Before mounting the vehicle on the chassis dynamometer the appropriate flywheel combination was determined and locked in place to simulate the inertial load of the vehicle. The inertia setting for the bus was equal 44,000 lbs. The outer rear wheel on the drive axle is removed and fitted with hub adapters which are later connected to the face plate. The vehicle was backed onto the dynamometer and the vehicle drive axle which drives the flywheel assembly and power absorbers were connected through a hub adapter. The vehicle was leveled with the drive axle and the tires were checked for any distortion as it would add to the vehicle loading. The vehicle exhaust was now connected to the dilution tunnel via insulated transfer tubes. The vehicle was chained down to the dynamometer bed as a safety measure.

The vehicle was made to run at a high speed after being mounted on the dynamometer to warm the lubricating oil in the differentials. This was done to reduce additional load on the vehicle due to highly viscous oil. During warming up of the differentials the gas analyzers were zero-spanned with blower operating at set-point. The driver interface speed monitor and communication head sets were put in place to aid the driver in following the scheduled drive cycle. A dummy test was conducted by making vehicle to run over the scheduled drive cycle with dummy media loaded in the tunnel to check whether the gas analyzers operated within the range for which they were calibrated and to check the flow through the mass flow controllers. If the analyzers pegged or measured below the range then they were recalibrated with proper span gas and the mass flow controllers were checked for any malfunction. After the warm up run the vehicle was shut down and allowed to soak for twenty minutes. During the soak time the official media required for various sampling were loaded in their respective holders and mounted onto the tunnel. The media loading was carried out in the controlled chamber to avoid accumulation of dust or other debris, a set of field blanks were maintained to study the effect of transportation on the used and unused media.

This study was unique for the fact that the work plan required adequate mass collection on the thermally denuded and non-denuded filters for toxicity and mutagenicity assays. The toxicity analysis required 1mg loading on the filters and the mutagenicity assays required 0.5mg loading on the filters. However, natural gas PM consisting predominantly of organic fraction, would be completely devoid of any mass in the thermally denuded sample. Hence, the test matrix was decided to be based on the mass loading on the filters of the non-denuded stream.

Initial test runs were conducted to infer the PM mass emissions from the test vehicles. Due to the lack of accurate weighing capabilities on field, the number of hours of cycle repetitions was decided based on the initial test runs for each cycle. Table 6 below summarizes the number of repetitions of the individual cycle to attain adequate mass loading.

Table 6 Cycle repetitions for PM mass loading

Test Cycle	Cycle Duration (Min)	Number of Repetition
3x UDDS	53	10
Idle	60	13
45 MPH	60	12

Vehicles were repeatedly exercised over their respective drive cycles for the stipulated number of testing hours to collect PM onto the filters. The filters were not replaced and mass from consecutive testes were repeatedly loaded onto the same filters. Decision to extend the test matrix, if required were made based on approximate and unconditioned weighing of the filters at the Stockton, CARB facility. Unregulated sampling streams were sampled over three repetitions of each cycle. Tunnel blanks and system blanks were collected for all sample streams at the end of each testing day. Figure 12 and Table 7 summarizes the different special sampling streams with their respective sampling instruments and flow rate settings.

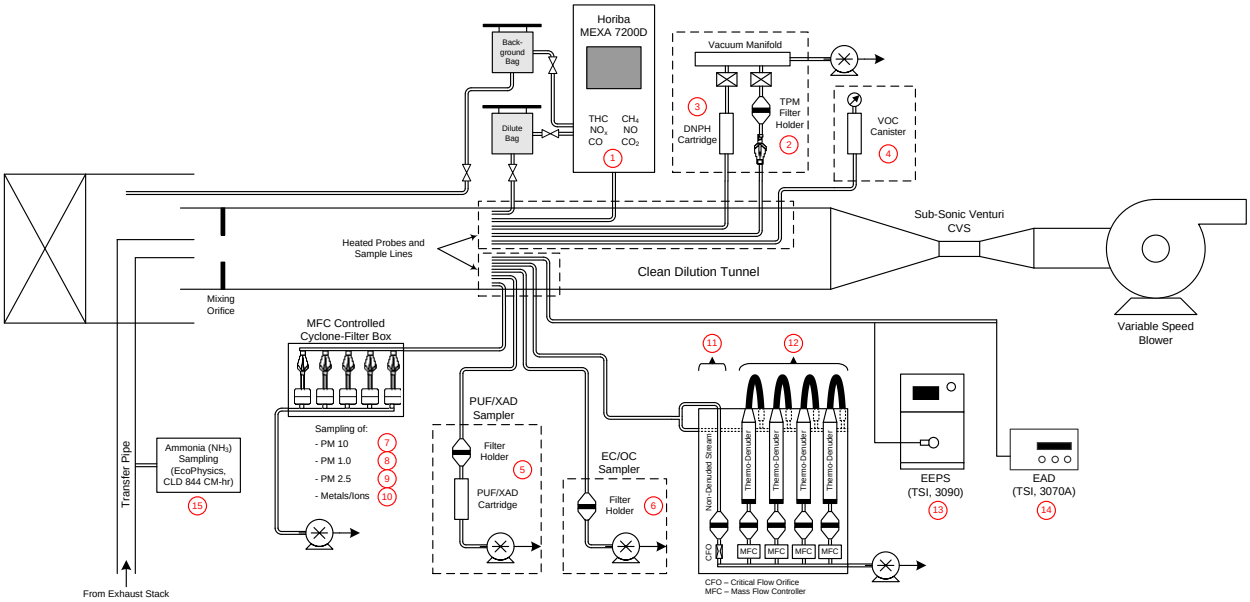

Figure 12 CVS and media sampling setup

Table 7 Summary of sampling media, sampling device and methods used to analyze unregulated exhaust species

ID	Sample	Media Type	Flow rate/ Flow Control
Unregulated Sampling			
3	Carbonyls	DNPH cartridge	2 lpm, Critical flow orifice
4	VOC	Steel Canister	Critical flow orifice provided by MLD
5	PAH	PUF/XAD and 90mm T60A20	200 lpm, Critical flow orifice
6	PM 2.5 EC/OC	Pre-fired Quartz (WVU Critical flow Cyclone Sampling)	16.7 lpm (2.5 micron URG Cyclone)
9	PM 2.5 Ions	Teflon (WVU Critical flow Cyclone Sampling)	16.7 lpm (2.5 micron URG Cyclone)
10	PM 2.5 Metals	Teflon (WVU Critical flow Cyclone Sampling)	16.7 lpm (2.5 micron URG Cyclone)
13	Particle Size Dist.	Transient EEPS, EAD	10 lpm

ID	Sample	Media Type	Flow rate/ Flow Control
Toxicity Sampling			
11	Toxicity stream with Volatiles	47mm T60A20	200 lpm, Critical flow orifice
12	Toxicity stream w/o Volatiles	47mm T60A20 through the Thermodenuder System	50 l/min/ denuder stream, mass flow controller
11	Ros Tox	47mm T60A20	2.5 scfm, mass flow controller
11	Mutagencity	47mm T60A20	2.5 scfm, mass flow controller

4.6 EMISSIONS CALCULATIONS

4.6.1 Equations to Calculate Distance Specific Mass of Exhaust Species

The equation used in calculating the distance specific emissions of unregulated components is similar to the equation used in calculating the regulated emissions. The emissions levels of unregulated species were analyzed by Environment Canada, which were later used to obtain the distance specific emissions.

The chemical speciation analysis was performed by calculating the total volumetric flow through the tunnel. The total flow through the tunnel is given by:

$$V_{Tunnel} = \left(V_{mix} + V_{\min i} + V_{PUF/XAD} + V_{DNPH} + V_{VOC} + V_{Denuder} + V_{PM1.0} + V_{PM2.5} + V_{PM10}\right) \quad \textbf{(Eq. 3.14)}$$

Where:

V_{Tunnel} = Total tunnel flow before removing the samples, in scf

V_{mix} = Total flow through the tunnel with samples removed for analysis, in scf

V_{mini} = Total flow through the secondary dilution tunnel, in scf

$V_{PUF/XAD}$ = Total flow through the PUF/XAD cartridge, in scf

V_{DNPH} = Total flow through the DNPH cartridge, in scf

V_{VOC} = Total flow collected into VOC canisters, in scf

$V_{Denuder}$ = Total flow from denuded and non-denuded stream, in scf

$V_{PM1.0}$, $V_{PM2.5}$, $V_{PM10.0}$ = Total flow through the respective cyclones, in scf

The flow ratio is the ratio of the total tunnel flow to the total sample flow of the respective sample being removed from the primary dilution tunnel.

$$V_{ratio} = \frac{V_{Tunnel}}{V_{Sample}} \qquad \textbf{(Eq. 3.15)}$$

The methods used in analyzing the emissions levels of the unregulated species and the equations used to calculate the distance specific emissions is discussed in the following sections.

4.6.1.1 Volatile Organic Hydrocarbons

The concentration of the methane, non-methane and other volatile organic compounds was used in the following equation to obtain the total emissions in grams/mile.

$$X_{emitted} = X_{Conc} \cdot V_{Tunnel} \cdot \frac{1}{L} \cdot 10^{-6} \qquad \textbf{(Eq. 3.16)}$$

Where:

$X_{emitted}$ = Total methane or non-methane hydrocarbon emitted by the test vehicle (g/mile)

X_{Conc} = VOC concentration obtained during GC analysis (ng/L).

V_{tunnel} = Total flow through the tunnel before removing the samples, in L

4.6.1.2 Semi Volatile and Particle Bound Hydrocarbon Analysis

During the test procedure, a PUF/XAD canister and 70mm filters were placed in series to collect semivolatile and particle-bound organic compounds. After the test, the media cartridge was removed from the sleeve in a dimly lit area and the ends were covered with aluminum foil to prevent any measurement errors due to secondary reactions. Analysis of the species thus obtained was performed through extraction and column fractionation.

The concentrations obtained during the analysis were used to determine the distance specific emissions of the individual PAH compounds from the test vehicle via the following equation:

$$X_{emitted} = X_{mass} \cdot V_{ratio} \cdot \frac{1}{L} \cdot 10^{-6} \qquad \textbf{(Eq. 3.17)}$$

Where:

$X_{emitted}$ = Distance specific emissions from the test vehicle (g/mile).

X_{mass} = Mass of PAH compounds inferred from the analysis procedure (μg).

5 RESULTS AND DISCUSSIONS

5.1 REGULATED EMISSIONS

A summary of the regulated emissions from the two buses tested over the three different test cycles are shown in Figure 13 and Figure 14. Figure 13 represents the regulated emissions as work specific and Figure 14 represents the regulated emissions as distance specific. The emissions from the chassis laboratory are usually represented as distance specific, however due to the availability of hub work (ahp-hr) the results are also represented in a work specific format. The work specific results can be used as an indication of the vehicles emissions limits with respect to its certification values. Results are presented as averaged results of number of tests that satisfy a COV of 5% for CO_2 emissions. The error bars indicate the maximum and minimum emission values of the averaged tests. The CO_2 are scaled down by a factor of 100 for ease of data plotting. Idle emissions are plotted as g/sec and scaled by a factor of 100 for ease of plotting. The hydrocarbon (HC) plotted in the chart represents Total Hydrocarbons (THC). The presence of an oxidation catalyst reduced the concentration of Non-Methane Hydrocarbons (NMHC) to very low levels, and hence the THC concentrations were very close to the methane concentrations. THC values are plotted to avoid reporting very small and in some cases negative NMHC values.

Regulated emissions were sampled over a triplicate length UDDS cycle. The 2010 compliant ISL G-280 Cummins CNG engines are stoichiometrically fueled, 3-way catalyst equipped engines. The 3-way catalyst is effective in reducing NO_x emissions with stoichiometric fuelling. Axle-work specific NO_x emissions from the vehicles were close to certification limit of 0.20 g/bhp-hr NO_x emissons. However, it is to be noted that certification values are calculated to work available at flywheel, and the chassis dynamometer calculates work available at the wheels. Engine work would be significantly higher than the work available at wheels due to transmission inefficiencies and loading from auxiliary systems such as air compressors.

NO_x emissions from bus 2 were 30% lower than bus 1 emissions over the UDDS cycle. This could be due to the differences in catalytic activity in reducing NO_x emissions. Further the difference in catalytic activity is also observed in the emissions of CO and THC from the two buses. Bus 2 was observed to emit 49% lower CO emissions than bus 1, similarly the THC emissions from bus 2 were 46% lower than bus 1. It is also to be noted that a 6% difference in CO_2 emissions over the UDDS cycle between the two buses indicate a very similar fuel

consumption. The PM emissions from bus 2 were 52% greater than of bus 1. CNG vehicles are usually characterized by low PM mass emissions due to the higher organic carbon or volatile carbon fraction of PM. A major portion of the PM emissions from a natural gas vehicle is attributed to entry of lubrication oil into the combustion chamber. The observed results could indicate a higher lubrication oil effect on bus 2 in comparison to bus 1.

NO_x emissions were close to detection limits, during the 45MPH steady state cycles, due to a steady fuelling rate. Stoichiometric engines are usually characterized by slight oscillations in air-fuel ratio in a narrow band between rich and lean mixture. This is usually done to better optimize the NO_x, CO and NMHC reduction capabilities of the 3-way catalyst. NO_x and NMHC are better reduced with a slight rich mixture and CO with a lean mixture. This varying air-fuel ratio is better controlled during a cruise mode operation hence resulting in lower NO_x emissions.

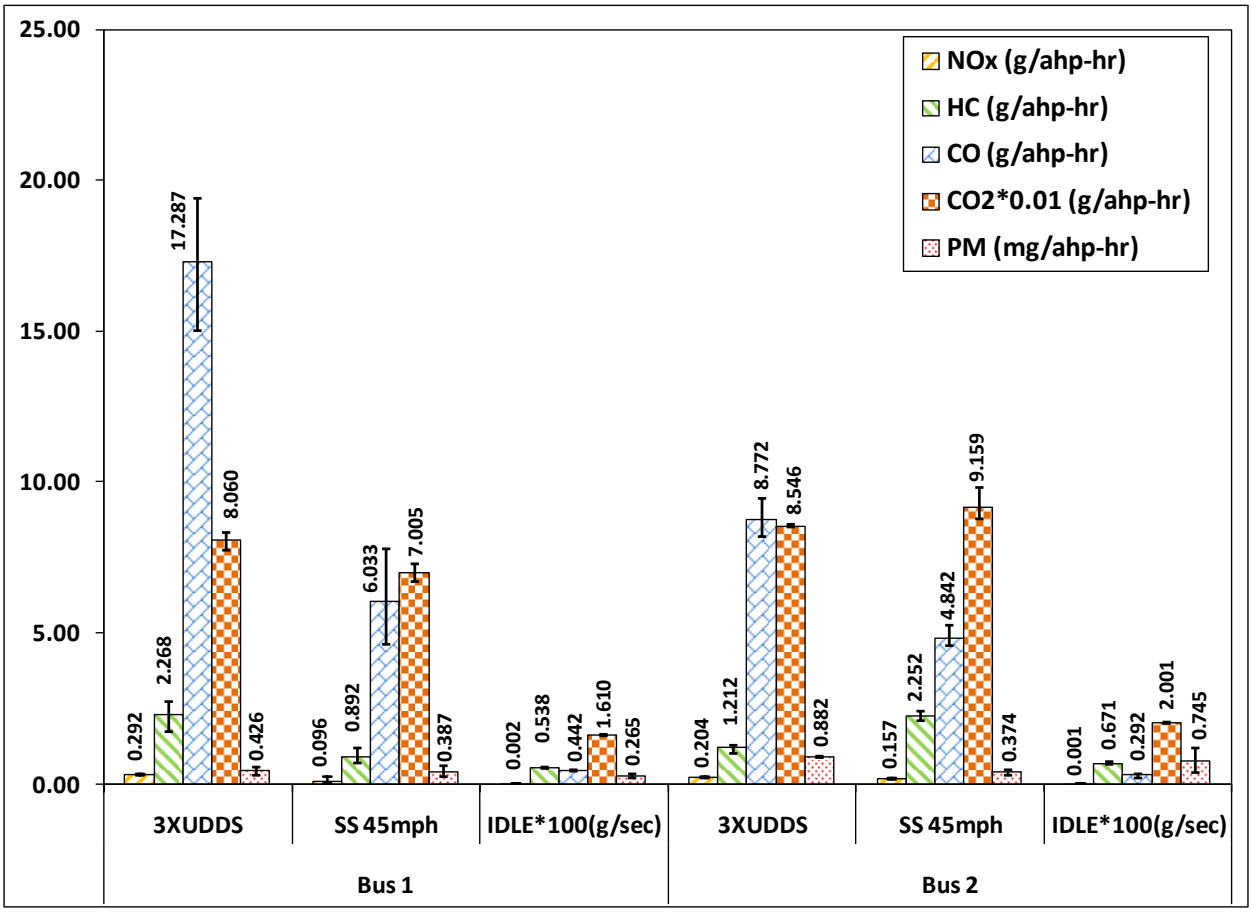

Figure 13 Work specific regulated emissions summary of test vehicles over the different test cycles

The PM mass emission on idle mode from bus 2 was 64% higher than bus 1. This could be attributed to the increased lubrication oil consumption of the bus 2. Although both buses were of similar in mileage bus 2 had about 8000 miles in excess of bus 1. The differences in mileage could be attributed to the differences in PM emissions, especially during idle modes, which are characterized by low in-cylinder pressures and consequently ineffective sealing of the combustion chamber by the piston rings.

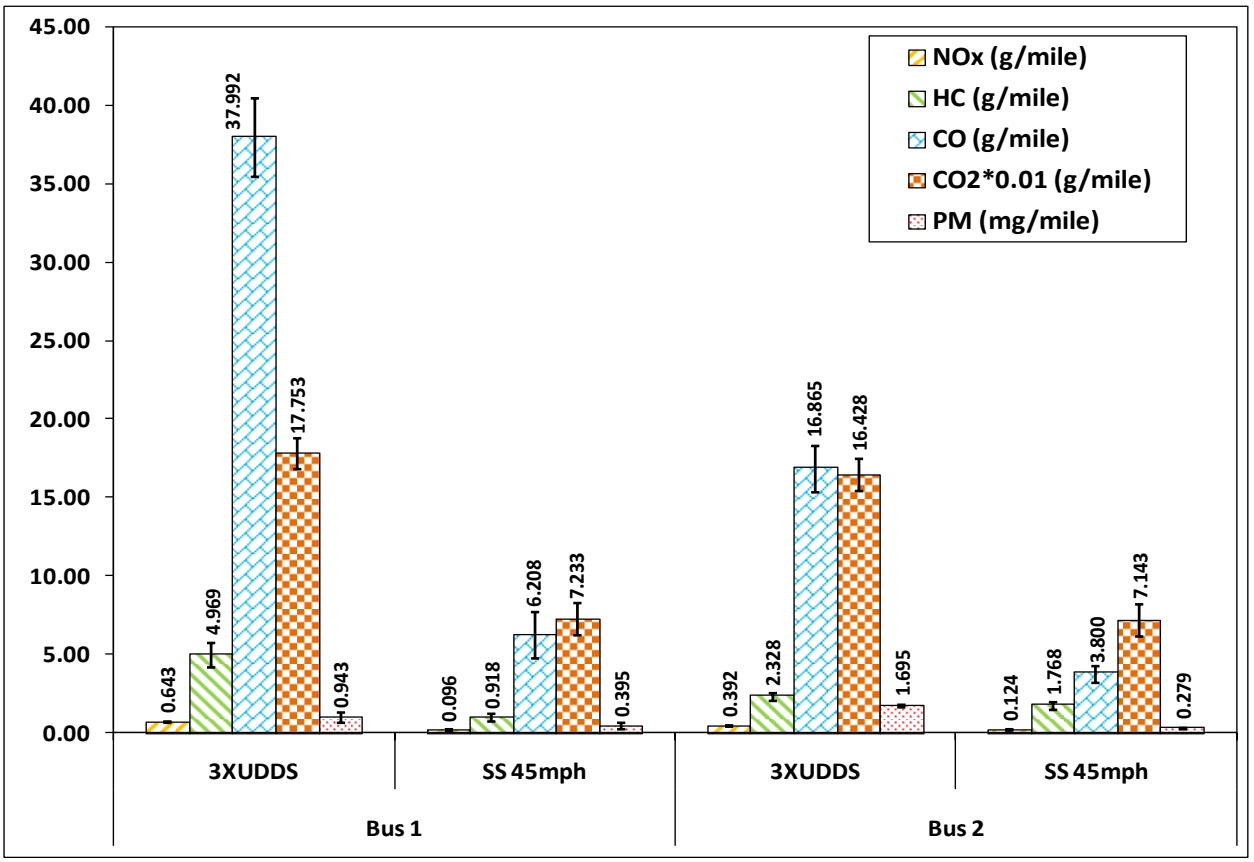

Figure 14 Distance specific regulated emissions summary of test vehicles over different cycles

Oxidation catalysts have a better catalytic activity towards NMHC in comparison to methane. Methane usually requires sustained high exhaust temperatures for complete catalytic light-off. The continuous THC readings were very close to the continuous methane readings, indicating a complete removal of NMHC compounds by the catalyst.

5.2 CRITERIA POLLUTANT COMPARISON WITH PREVIOUS STUDIES

Criteria pollutants emissions from this study were compared to emissions from CNG and diesel buses equipped with DPF and SCR studied previously to illustrate the differences in emissions as a result of after-treatment systems and vehicle technology.

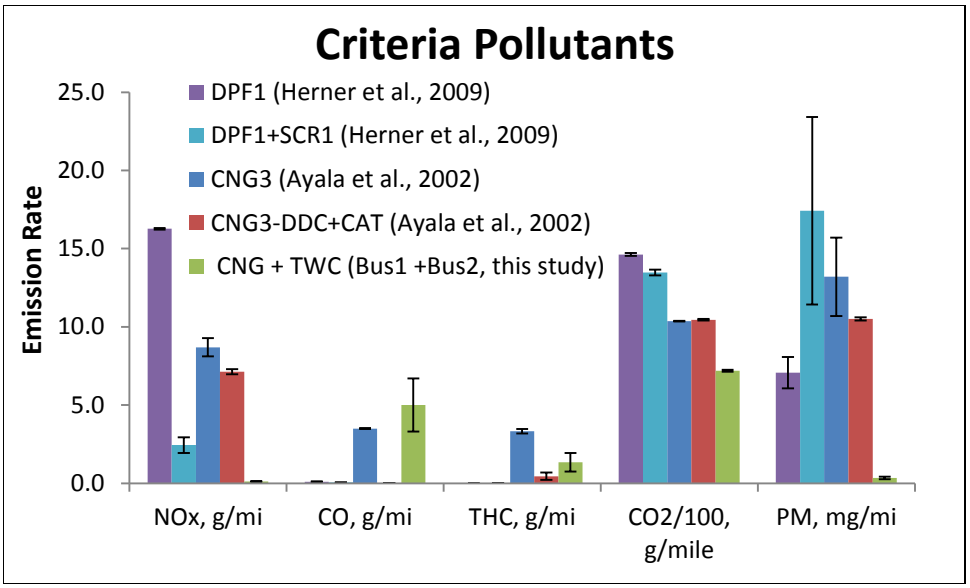

Figure 15 Cruise mode criteria pollutant comparison between current and previous studies

Figure 15 shows the emissions comparison between TWC equipped CNG buses (CNG+TWC) tested in this study with DPF equipped diesel bus (DPF1), DPF-SCR retrofitted diesel bus (DPF1+SCR1), baseline CNG bus (CNG3) and CNG bus equipped with oxidation catalyst (CNG3-DDC+CAT). DPF1 bus was equipped with Johnson Matthey CRT, consisting of a DOC followed by an uncatalyzed DPF, SCR1 was a prototype vanadium based catalyst, and the baseline CNG vehicle was powered by MY 2000 DDC Series 50 CNG engine operating on lean-burn technology [74, 75]. It is to be noted in this comparison that the cruise mode speeds in the various studies are not the same. The current study tested the vehicle at 45 MPH and Herner et al., and Ayala et al. used speeds of 55 MPH and 50 MPH respectively. We assume the effect of the vehicle speed on the criteria pollutants emission could be insignificant.

The TWC catalyst equipped stochiometrically fueled buses (CNG+TWC) show almost complete reduction in NOx emissions; however NOx emissions from CNG3 vehicles are of the same order of magnitude in comparison to diesel vehicles without SCR systems. SCR retrofit system on the DPF1 vehicle contributes to 85% decrease in NOx emissions from its baseline

configuration. The 2010 compliant CNG buses prove to be a great alternative fuel technology capable of meeting current USEPA NOx regulations.

Stoichiometric operation of the TWC equipped CNG bus resulted in higher CO and THC emissions in comparison to the lean-burn technology OC equipped CNG vehicles.

The CNG+TWC vehicle also exhibits significant PM benefits in comparison to CNG3-DDC+CAT vehicles. Although, lubrication oil combustion has proven to increase mass emissions of PM from CNG vehicles, their effect is more pronounced in transient and idle mode operations.

5.3 UNREGULATED EMISSIONS

The study involved the speciation of carbonyl, poly aromatic hydrocarbons compounds (PAH), elemental carbon/organic carbon (EC/OC) and volatile organic compounds (VOC). PAH compounds were extracted and quantified by South West Research Institute (SWRI) and carbonyl, EC/OC and VOC were analyzed by Monitoring Laboratory Divisions (MLD) of CARB. Raw data reported by the different institutions were reduced with tunnel flow rates to calculate grams of species in the dilution tunnel.

The results are reported uncorrected for background, with background values plotted separately as tunnel background concentrations. This method has been adopted to avoid reporting negative background corrected test values in cases of concentrations with high measurement uncertainty due to measurement close to or below detection limit.

5.3.1 Poly aromatic Hydrocarbons (PAH) Emissions

The PAH data contains speciation results of 22 different PAH compounds. List of target analytes were chosen to be the same as those quantified in previous phases of this study conducted by CARB. PAH compounds have major health impacts and EPA has classified these pollutants under the Hazardous Air Pollutants (HAP) category. PAH compounds are considered to be carcinogenic in nature. Emissions of PAH compounds are a characteristic of diesel exhaust, and these compounds are most often associated with PM emissions in diesel vehicles. However, their concentrations in CNG exhaust have found to be minimal and mostly arising from lubrication oil consumption. Sampling of PAH compounds are targeted towards three phases of existence of these compounds, namely gas phase, semi-volatile phase and particle phase. The gas

phase and semi-volatile phase are captured in the PUF/XAD cartridge and the particle phase is captured in the 90mm T60A20 upstream filter.

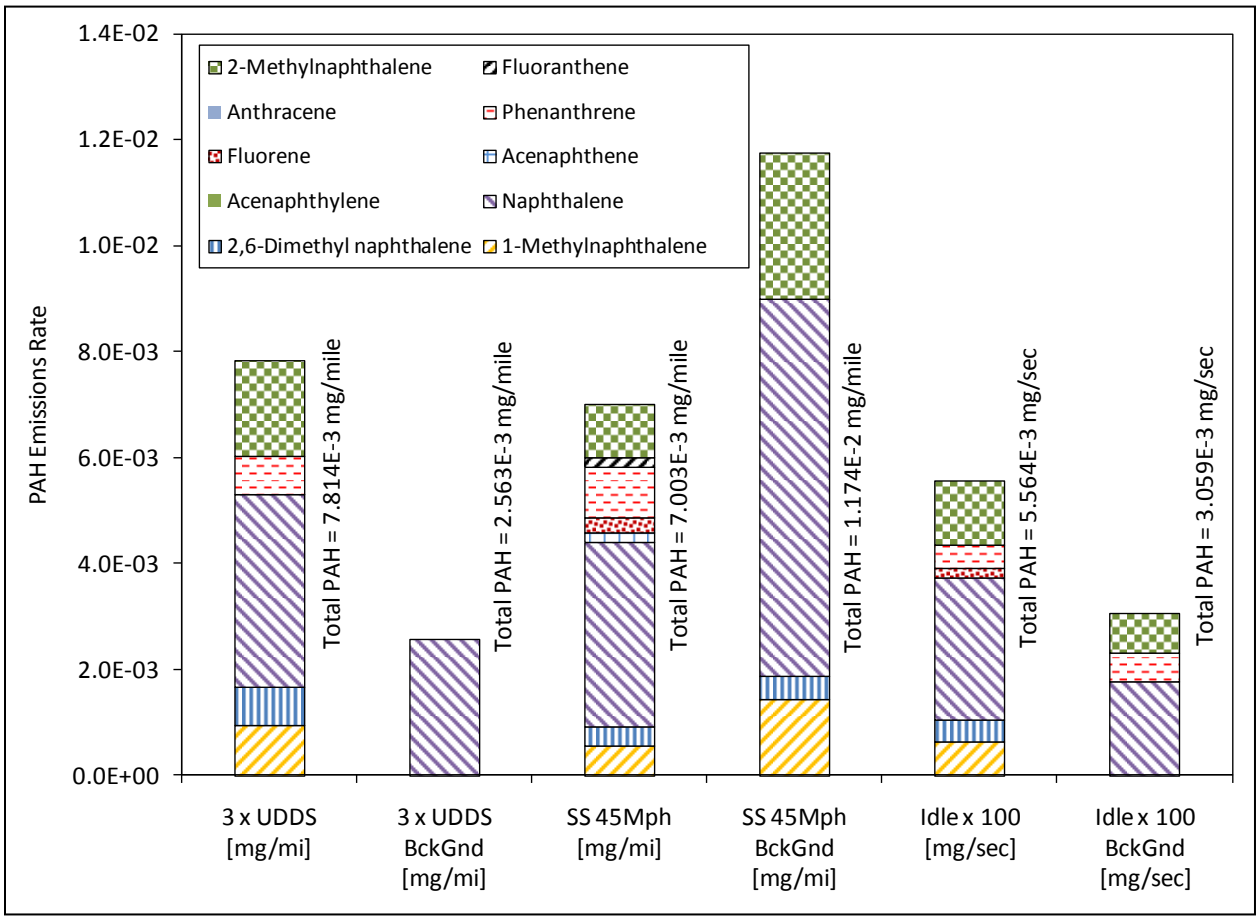

Figure 16 Distance specific (time-specific for Idle) PAH emissions results of CNG bus 1

Figure 16 and Figure 17 and represent the distance-specific PAH emissions of bus 1 and bus 2 respectively. Only analytes whose concentrations were found to be within the detection limits of the instruments have been reported. SWRI had assigned a zero concentration for analytes below detection limit.

The PAH emissions from the two buses were observed to be the same order of magnitude. With the absence of aromatic content in the fuel, the source of PAH emissions could be attributed to the lubrication oil consumption in the engine. Naphthalene was found to be the major contributor towards PAH emissions in both vehicles. Also, significantly high PAH concentrations were detected in the tunnel background samples. Similar observation was documented during in previous studies conducted in California.

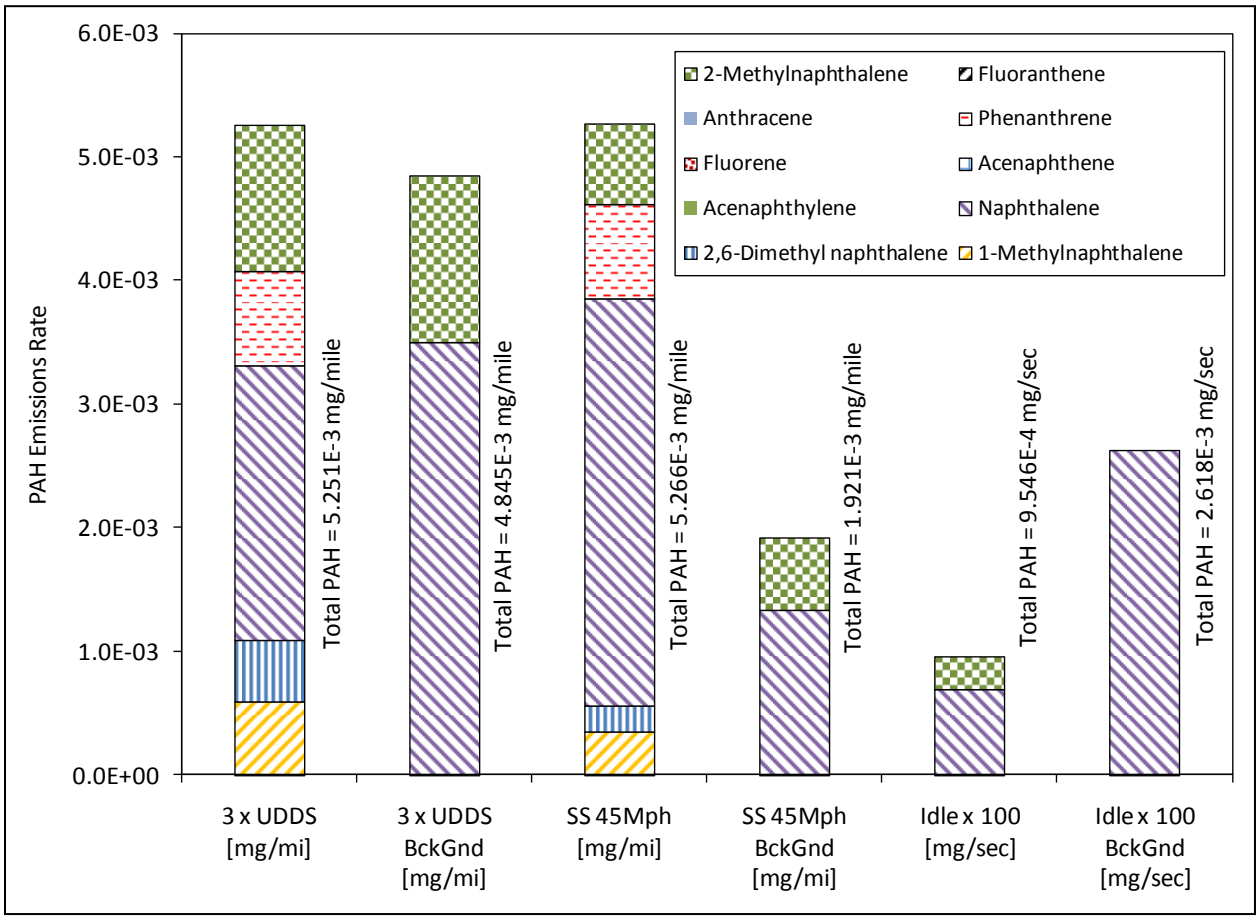

Figure 17 Distance specific (time-specific for Idle) PAH emissions results of CNG bus 2

5.3.2 Elemental Carbon / Organic Carbon (EC/OC)

EC/OC data was reported by CARB MLD. Samples were collected on to pre-fired quartz filters and shipped to MLD for EC/OC quantification. The analysis method involved the Thermal-Optical Reflectance (TOR) and Transmittance procedure. Thermal-Optical Transmittance procedure is based on the EPA/NIOSH method and reports a much detailed fraction of EC based on the transmittance of the filter [72]. The method quantifies 4 different OC fractions depending on the amount of CO_2 liberated at different temperatures and oxidizing environments. Also, reported is the EC fraction oxidized above 550°C. Together with these the reflectance method utilizes a laser and a photo diode to monitor the reflectance of the light non-absorbing OC and the light absorbing EC, to quantify the pyrolyzed portion of the OC depicted as RPOC in the chart [73]. Similarly, the transmittance method utilizes a laser photo diode and a photocell to detect the transmittance of the filter. Both the transmittance and reflectance aid in

correcting for the organic fraction that was pyrolyzed and converted to EC during the heat ramps. Also reported are Reflectance OC (ROC), Reflectance EC (REC), Transmittance OC (TOC), Transmittance EC (EC) and Transmittance Pyrolyzed OC (TPOC).

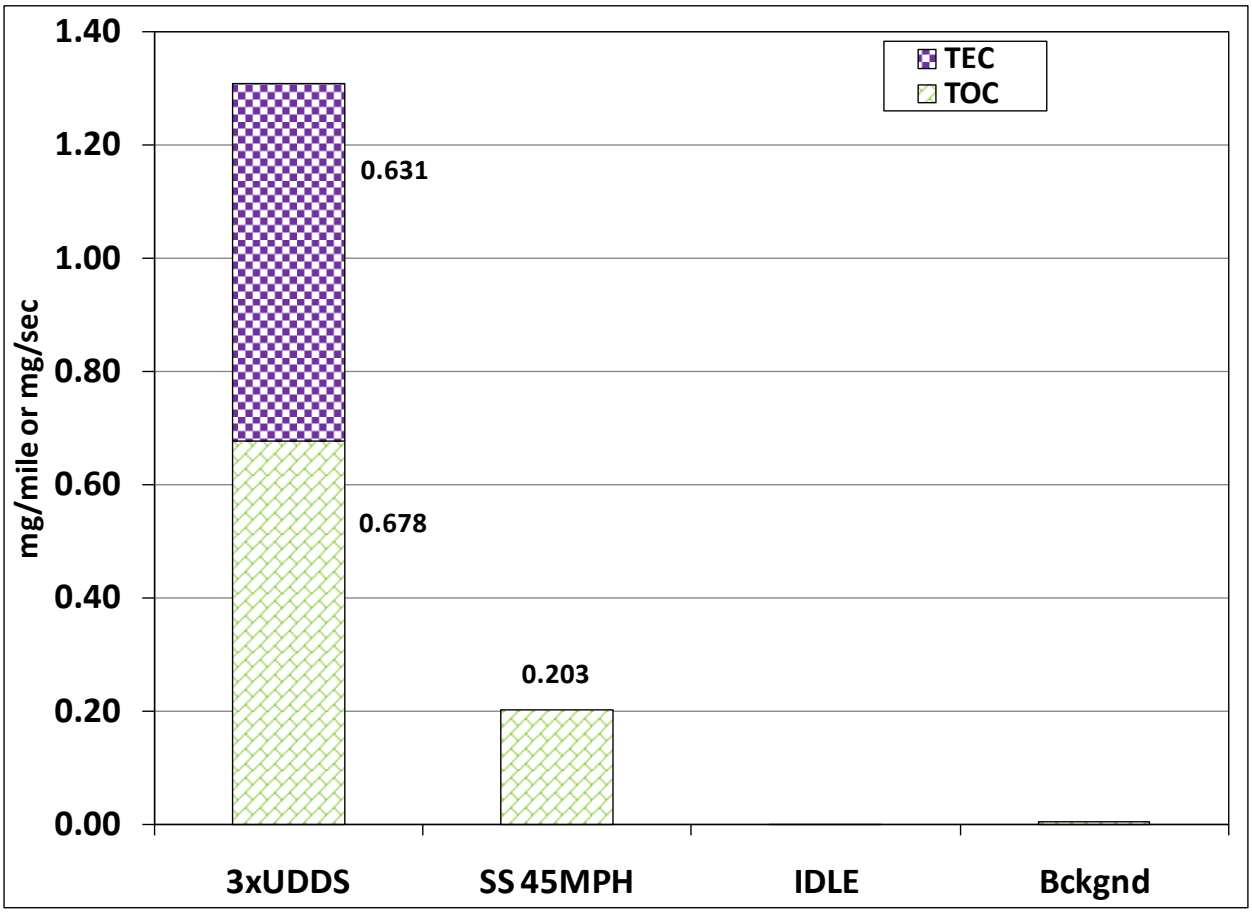

Figure 18 Distance specific EC/OC emissions results of bus 1

Figure 18 and Figure 19 show the distance specific EC/OC fractions of bus1 and bus 2 respectively. Results of all the different OC and EC quantification methods for a given cycle have been plotted. It can be seen that the PM from the CNG buses were completely organic in nature and is consistent with the established theory of CNG vehicles exhaust being completely or very minimal in EC concentrations. The TEC observed in the UDDS cycle of bus 1could be an outlier in the transmittance data. EC/OC emissions during the idle of bus 1 were observed to be close to background levels.

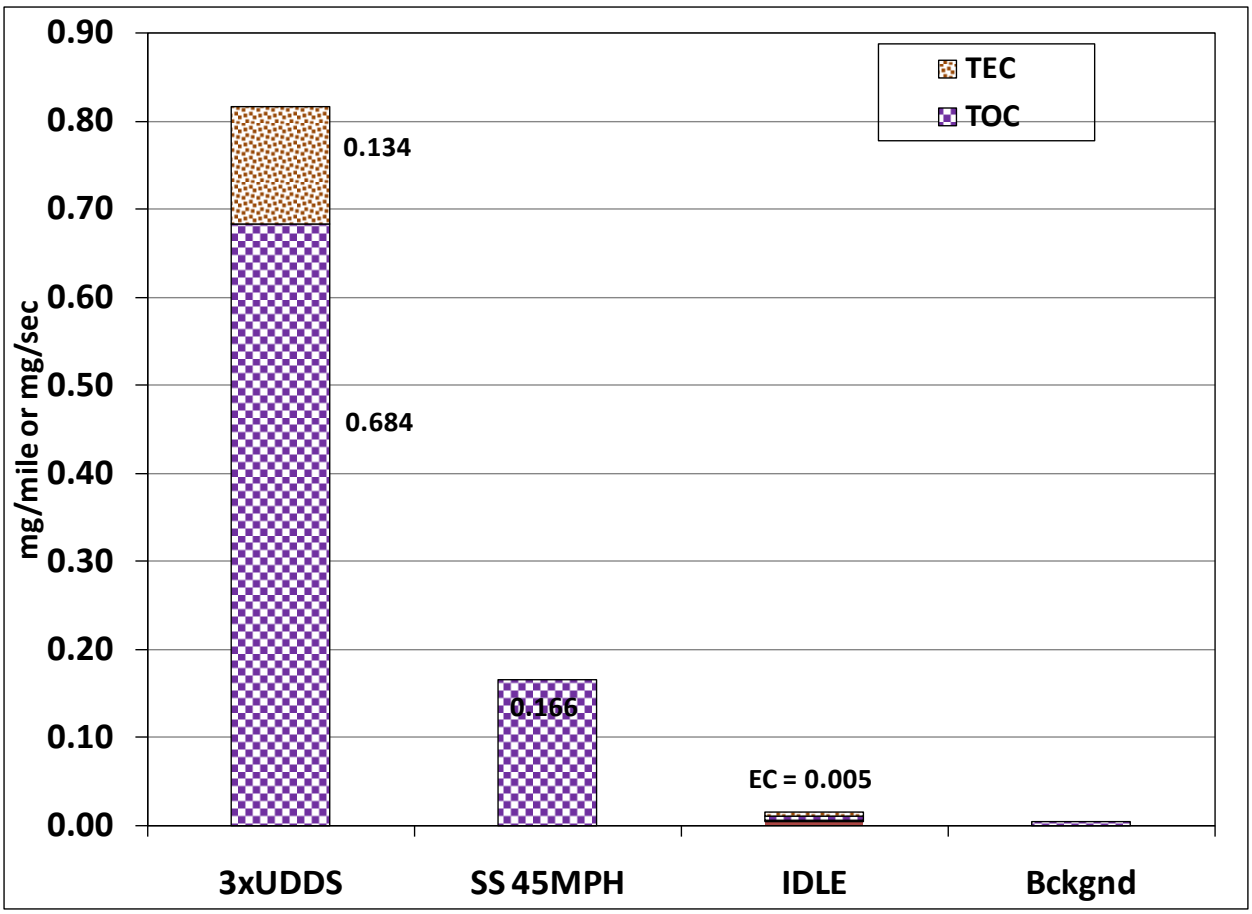

Figure 19 Distance specific EC/OC emissions results of bus 2

The organic fraction content of PM from bus 2 is similar to that observed in bus 1. A significant contribution in EC carbon is also observed and reported by the transmittance and the reflectance method. However, the thermal EC fraction was reported to be below detection limit. The source of the EC in these samples could be attributed to lubrication oil consumption, during the low speed, and idle modes of the UDDS cycle. Also, to support the argument 0.005mg/sec of EC fraction is also observed during the idle mode operation.

5.3.3 Volatile Organic Compounds (VOC)

VOC analysis was carried out and reported by CARB MLD. Further data post processing was performed by WVU to report distance specific VOC emissions. 28 different VOC compounds were quantified as part of the study. Concentrations reported to be below detection limits have been omitted in Figure 20 and Figure 21.

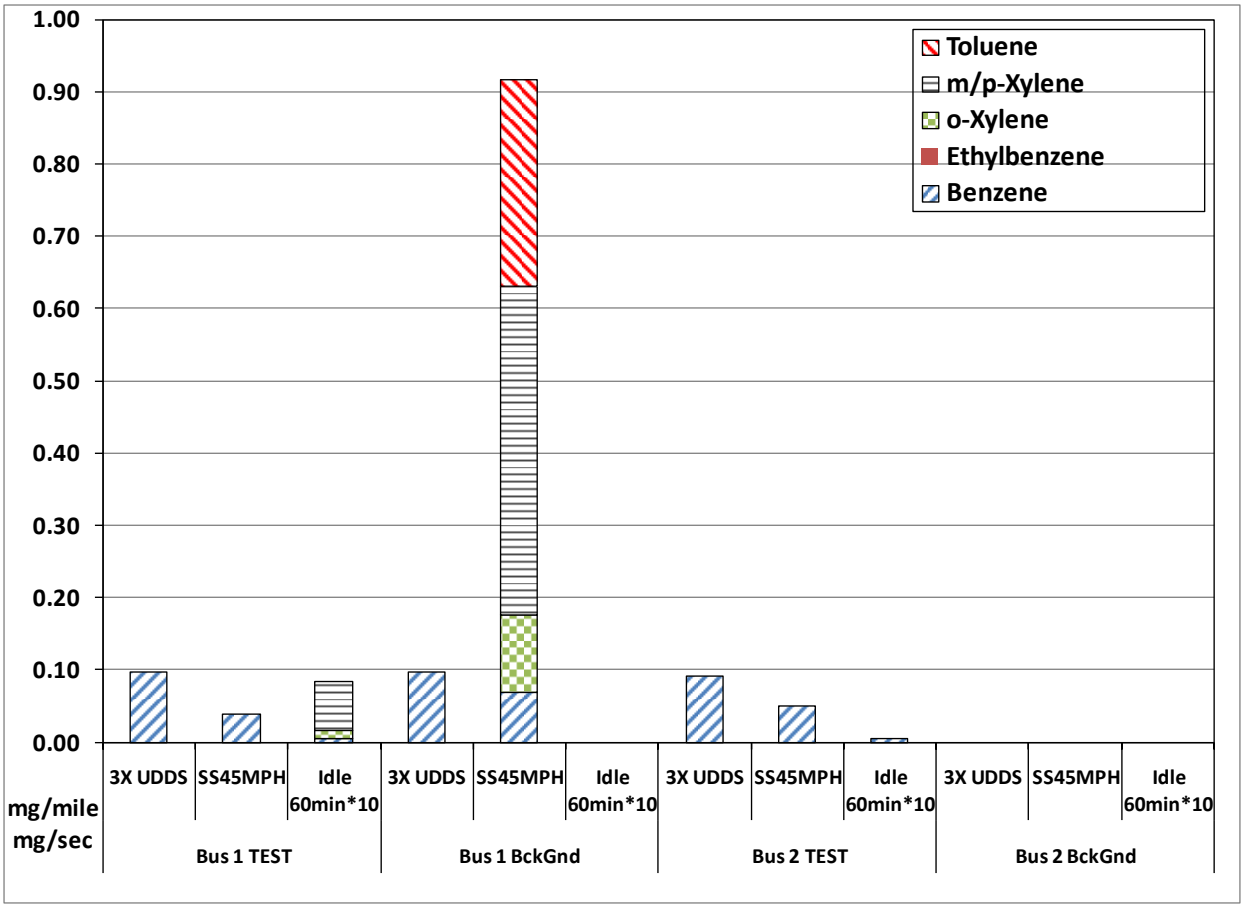

Figure 20 Distance specific BTEX emissions results from bus 1 and bus 2

Figure 20 shows the comparison of BTEX emissions between bus 1 and bus 2. BTEX compounds are part of the EPA list of hazardous air pollutants and indentified to be carcinogenic in nature, with mobile sources as their major source of emission. The presence of the 3-way oxidation catalyst after-treatment system was effective in reducing the concentrations of most BTEX compounds below detection limits. Oxidation catalyst are very effective in reducing higher-chain hydrocarbons over a wide temperature range unlike lower chain hydrocarbons which require higher exhaust temperatures for catalytic light-off. Most species test concentrations were lower or equal to background concentrations. However, high variations in background measurements were detected based on the time of day of background collection.

Figure 21 shows the comparison of ethanol, acrolein and acetone emissions between bus 1 and bus 2. Since all test concentrations are associated with high background values, the actual contribution of the exhaust to the concentrations of these species are very minimal. Also high

background variability due to time of data collection, introduces higher uncertainties in the actual vehicle exhaust emissions of these species.

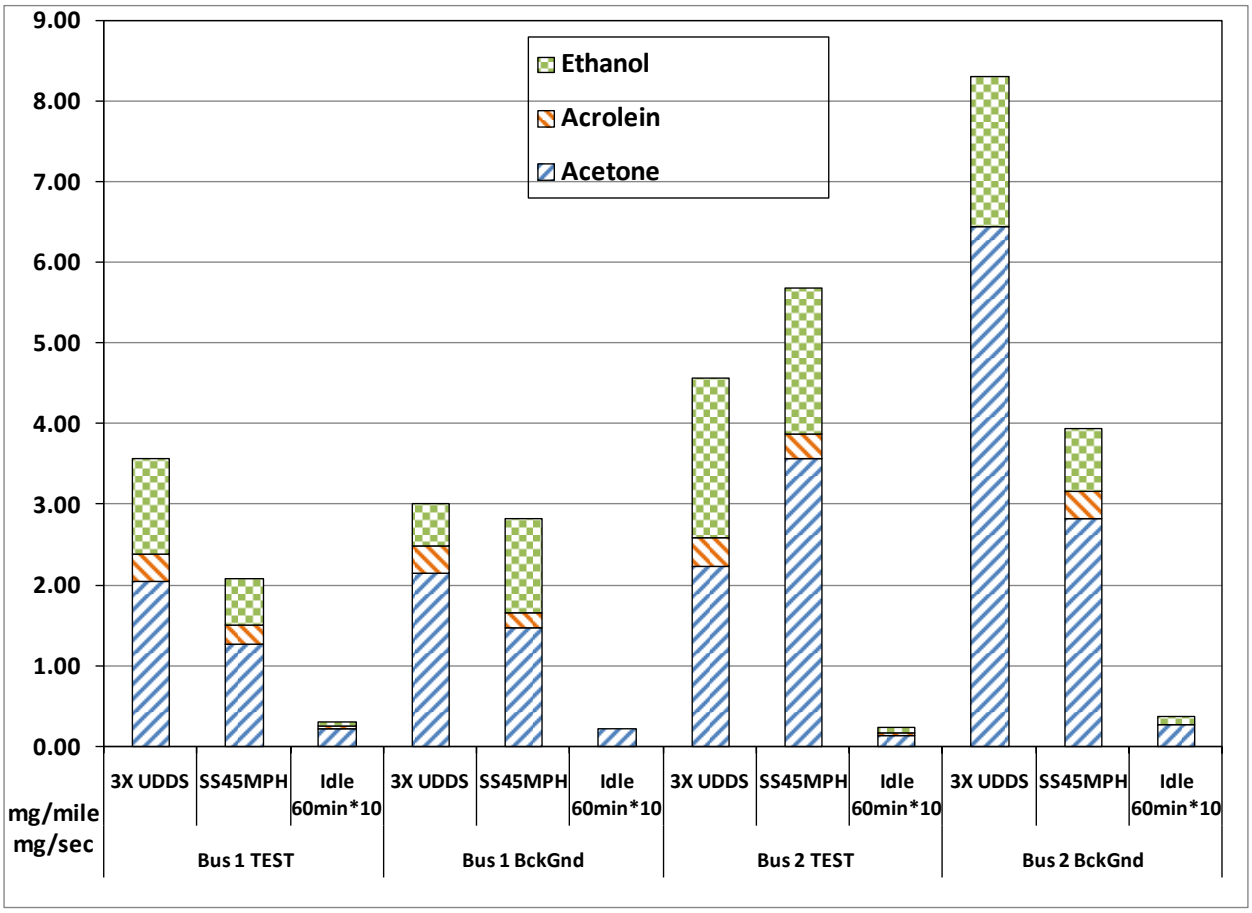

Figure 21 Distance specific VOC emissions of bus 1 and bus 2

5.3.4 Carbonyl Emissions

Carbonyl analysis was carried out by CARB MLD. Further data processing was completed by WVU to report distance specific emissions of the carbonyl species. Idle emissions and its background values are represented in units of mg/min. Species whose concentration were reported to below detection limits have been omitted from the chart. Figure 22 shows the distance specific carbonyl emissions from CNG bus 1 and bus2 over the three test cycles. Formaldehyde and acetaldehyde are commonly observed in significant concentrations in the exhaust of baseline CNG vehicles. However, oxidation catalysts have previously shown to reduce the concentration of most carbonyl species by over 90%. The TWC in the current study

has been effective in reducing both formaldehyde and acetaldehyde to levels found in background air. Since the vehicle in the current study was stoichiometrically fueled, exhaust temperatures were sufficient for sustained catalytic activity even in lower engine loads and idle conditions.

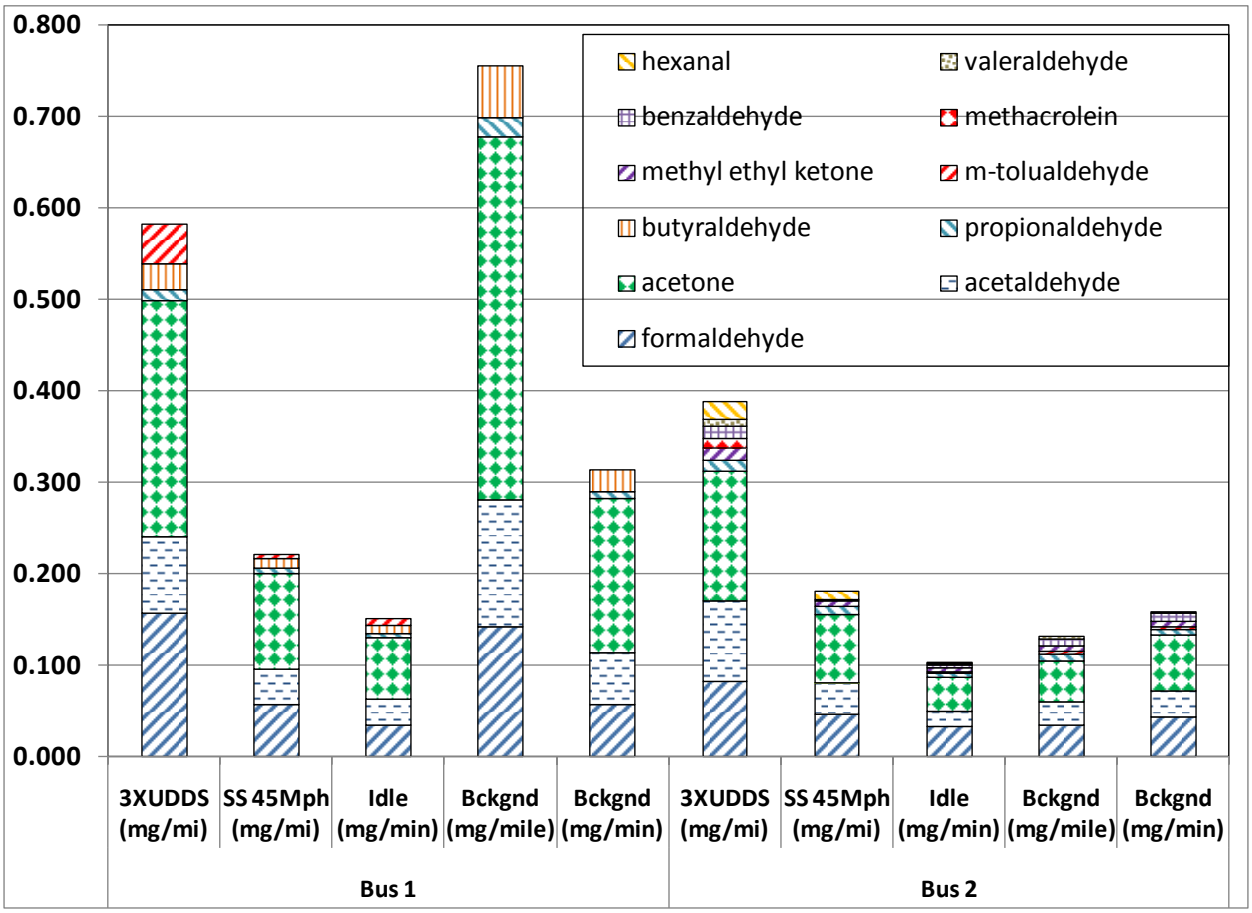

Figure 22 Distance specific (time-specific for Idle) Carbonyl emissions results of CNG bus 1 and 2

5.3.5 Water Soluble Ions Emissions

Ion analysis was carried out by University of Wisconsin laboratory and further data processing was performed by WVU to report distance specific emissions of the water soluble ions data. Figure 23 show the water soluble ions data for the two CNG buses tested in this study. The CNG fuel being completely devoid of sulfur, did not contribute to any sulfate formation. However, the results do not show a possibility of sulfate formation due to contribution from lubrication oil. All water soluble ions concentrations are close to levels found in the background. Since the concentrations detected were very low, it could be concluded that the water soluble ions results would contain a high level of measurement uncertainty. Although significant levels

of ammonia were detected in the exhaust, the presence of ammonium ions is close to background levels.

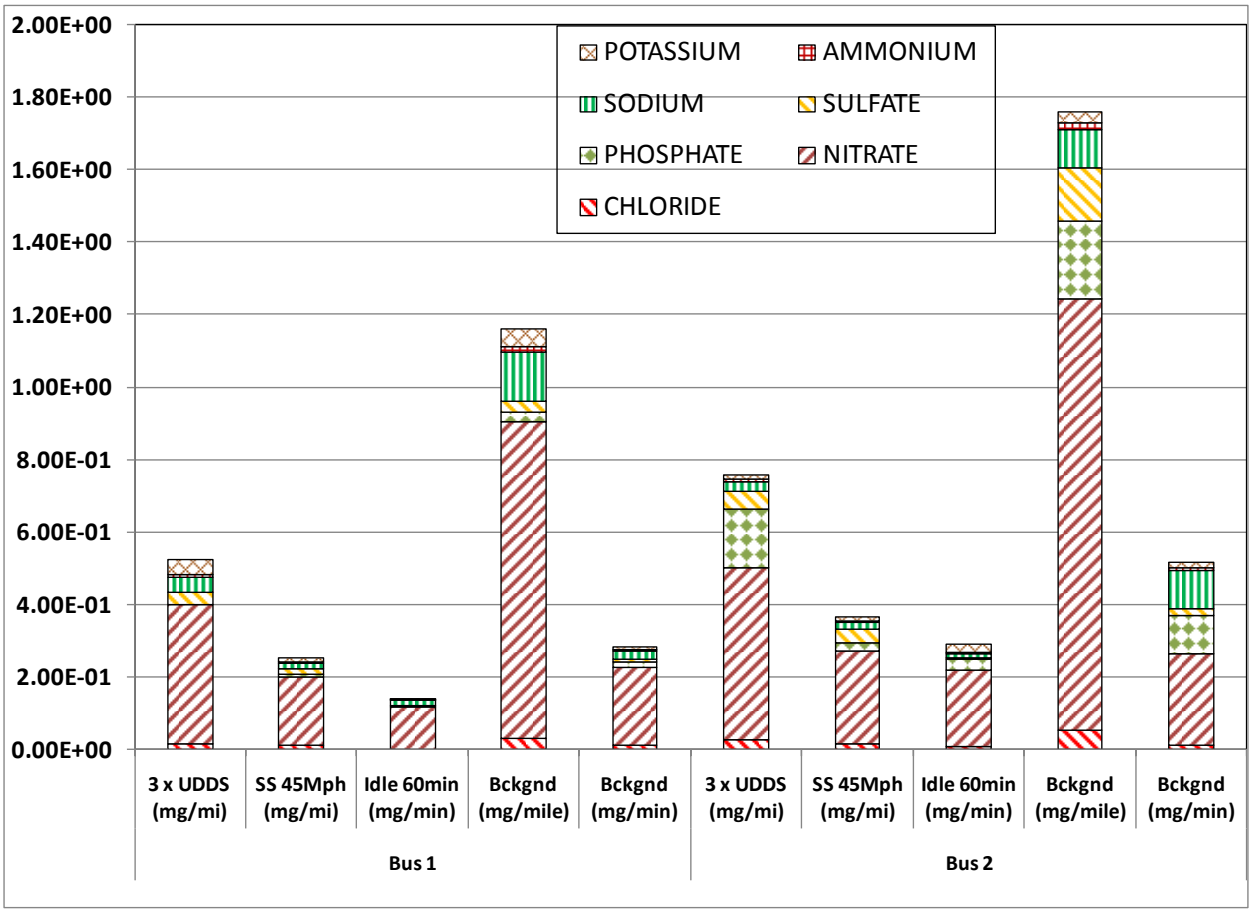

Figure 23 Distance specific (time-specific for Idle) water soluble ions emissions results of CNG bus 1 and 2

5.3.6 Metals Emissions

Metals analysis was performed by University of Wisconsin, laboratory and further data processing was carried out by WVU to present the data in distance specific units. Figure 24 shows the metals data for the two CNG buses tested in this study. UWM analyzed for 50 different elements, however due to the low concentrations of most metals, the chart displays a few commonly observed elements in heavy-duty vehicle exhaust. Calcium was detected relatively high in concentration both in test conditions and background samples. All metals were detected at concentrations close to background levels. Due to the low concentrations of elements detected the data would contain a high level of measurement uncertainty associated with it.

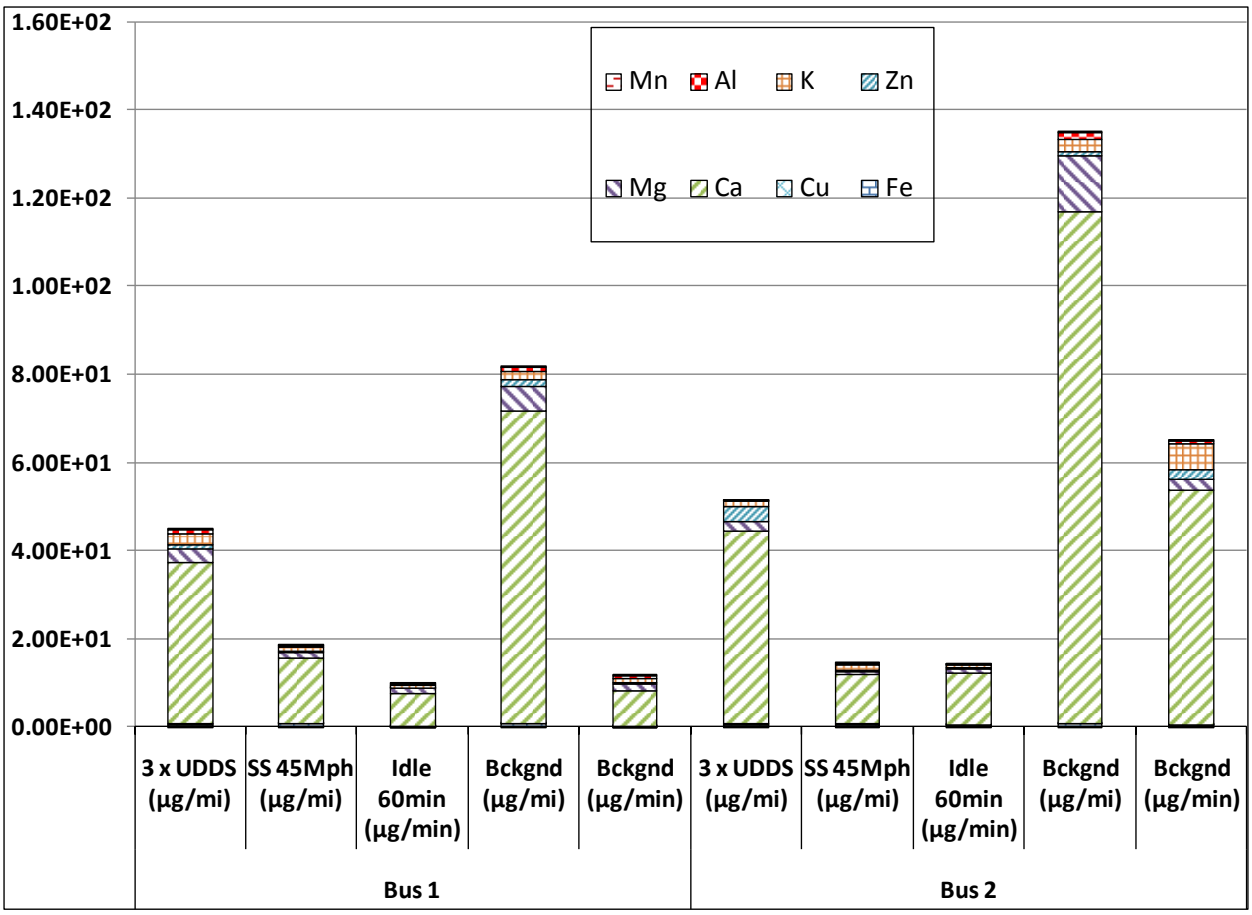

Figure 24 Distance specific (time-specific for Idle) metals emissions results of CNG bus 1 and 2

5.3.7 Particle Size Distribution and Concentration

The EEPS was setup for sampling from the CVS, and dilution ratios were calculated using carbon balance (see Section 3.6). The results of the particle sizing have not been scaled by the dilution ratio and hence they represent the concentrations observed in the CVS after dilution with the dilution air. Data has not been corrected with the dilution ratio, due to particle formation mechanism of CNG exhaust. The dominant particle formation mechanism of CNG exhaust would be either homogenous nucleation of hydrocarbons or sulfuric acid nucleation in the presence of high exhaust temperatures and suitable sulfate concentrations. Hence, the particles formed due to nucleation are not observed in the exhaust of the vehicle unlike accumulation mode which is a direct result of the in-cylinder combustion. Since, the number and size are dependent on the dilution conditions only, the results would be indicated with the dilution ratio and corrected for it.

The particle size distribution from the transient UDDS cycle has been represented as averaged number concentrations of the entire distribution during the cycle period. Error bars have been plotted to indicate the maximum and minimum variation in particle concentration over the entire size distribution. Figure 25 represents the size distribution and average particle concentration over the UDDS cycle of bus 1 and bus 2.

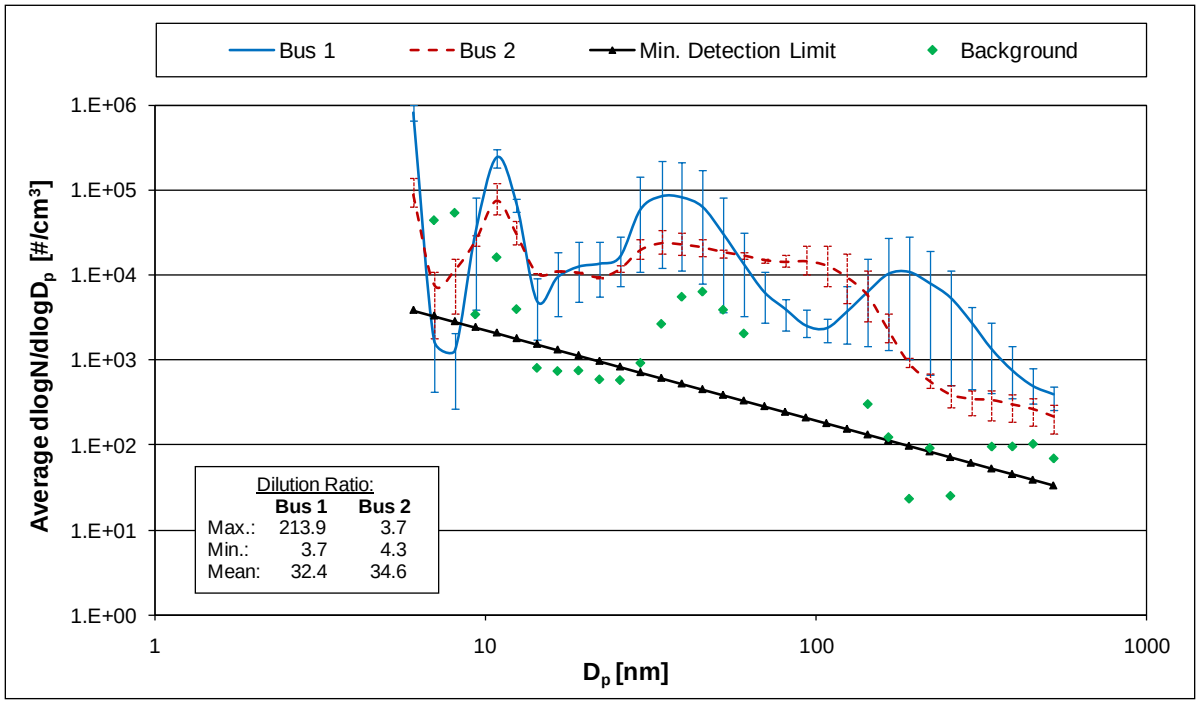

Figure 25 Average PM Concentration over triple-UDDS cycle, Sampled from CVS tunnel, No dilution ratio corrections, EEPS

The exhaust of CNG vehicles are characterized by higher concentrations of organic carbon than elemental carbon. This fact could also be observed in the EC/OC results of this study. The particle size distribution reflects a similar trend with a particle diameter peak of 10nm with minimal variation in particle number throughout the cycle. This 10 nm peak could be attributed to sulfates derived from lube oil nucleating with water to form sulfuric acid particles. Both buses represented a similar consistent 10 nm peak over the UDDS cycle. A comparison of gravimetric PM from both buses reveled higher PM emissions from bus 2 and a similar trend is reflected in the PM size distribution of bus 2 with a well defined accumulation mode with minimal variation in concentration over the transient UDDS cycle. The fact that the particle concentrations did not vary over the cycle, indicates that the source of these accumulation mode particles could be a result of consistent lube oil combustion.

Figure 26 represents the size distribution and average particle concentration over the 45MPH steady state cycle of bus 1 and bus 2.

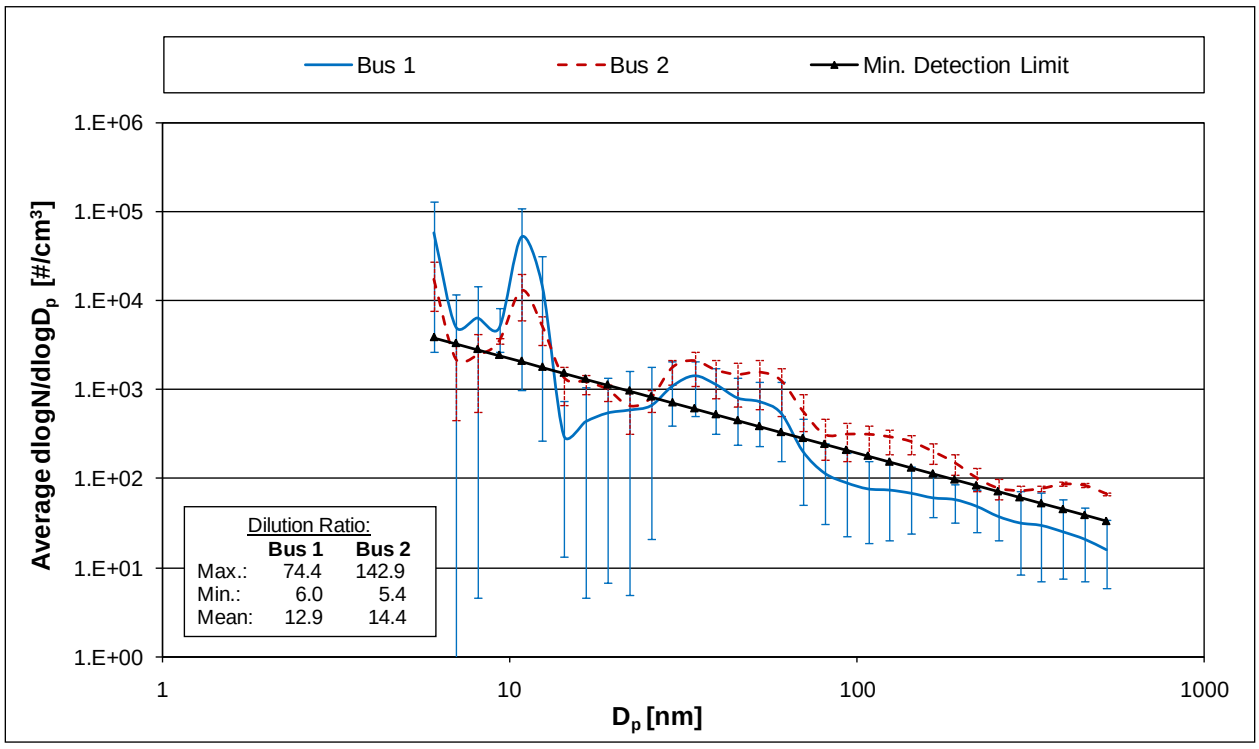

Figure 26 Average PM Concentration over 45Mph steady-state mode (60min), Sampled from CVS tunnel, No dilution ratio corrections, EEPS

The steady state cycle resulted in very low particle numbers that were close to the detection limit of the instrument, indicated by a solid line in the chart. The 10 nm peak observed in the transient cycle is also observed during the cruise cycle with the same order of magnitude in average particle number. However, a greater variability in particle concentration is also observed, due to measurement close to detection limits of the instrument.

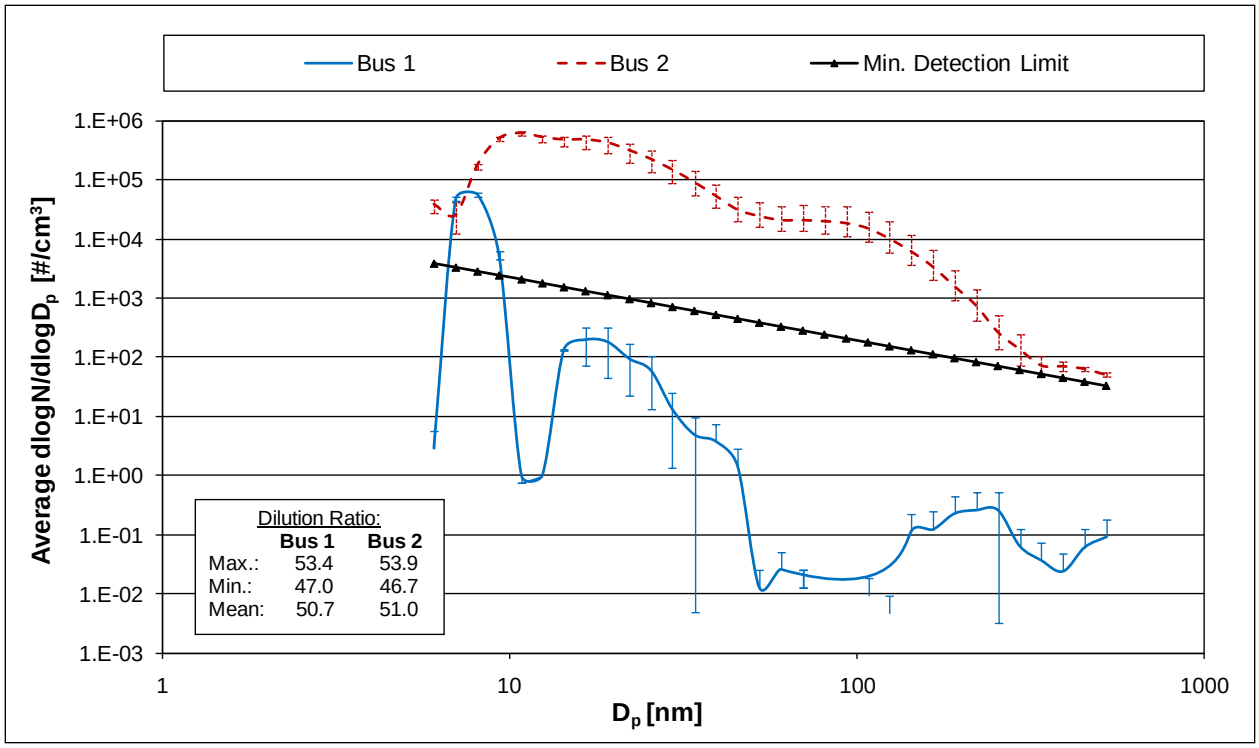

Figure 27 Average PM Concentration over Idle mode (30min), Sampled from CVS tunnel, No dilution ratio corrections, EEPS

Figure 27 represents the size distribution and average particle concentration over the idle mode of bus 1 and bus 2. Significant differences are observed in the particle size distribution and concentration from the idle mode operation of bus 1 and bus 2. Idle mode operation of bus 1 resulted in particle size distribution below the detection limit of the instrument. Bus2 size distribution exhibits a bi-modal distribution with a nucleation Count Mode Diameter (CMD) at about 10nm and an accumulation CMD of about 100 nm. As discussed above the source of nucleation mode could be as a result of sulfate nucleation from lube oil combustion. The possible reason for the presence of accumulation mode particle of 100nm in diameter is not clear. The EC/OC analysis did indicate the presence of EC on the sampled filters.

High PM loading was also observed on the toxicity PM filters. Figure 28 and Figure 29 show the pictures of the non-denude and thermally denuded toxicity filters sampled during idle mode testing. Higher PM loading from bus 2 could possibly be due to improper EGR metering which could result in excessive PM emissions during certain operating conditions such as idle and accelerations.

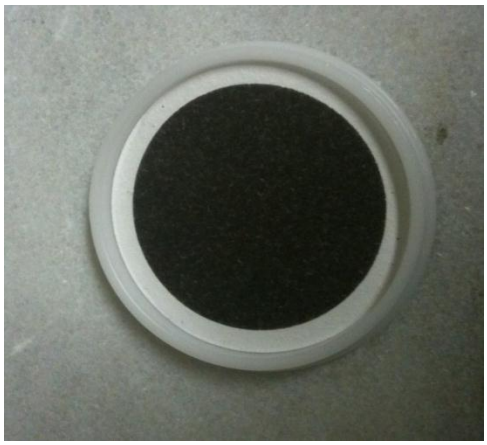

Figure 28 Non-denuded toxicity filters sampled during idle mode operation

Figure 29 Thermally denuded toxicity filters sampled during idle mode operation

Figure 30 represents the instantaneous total particle concentration during idle operation. It can be seen that the total particle concentrations from bus 2 were over a magnitude higher than bus 1.

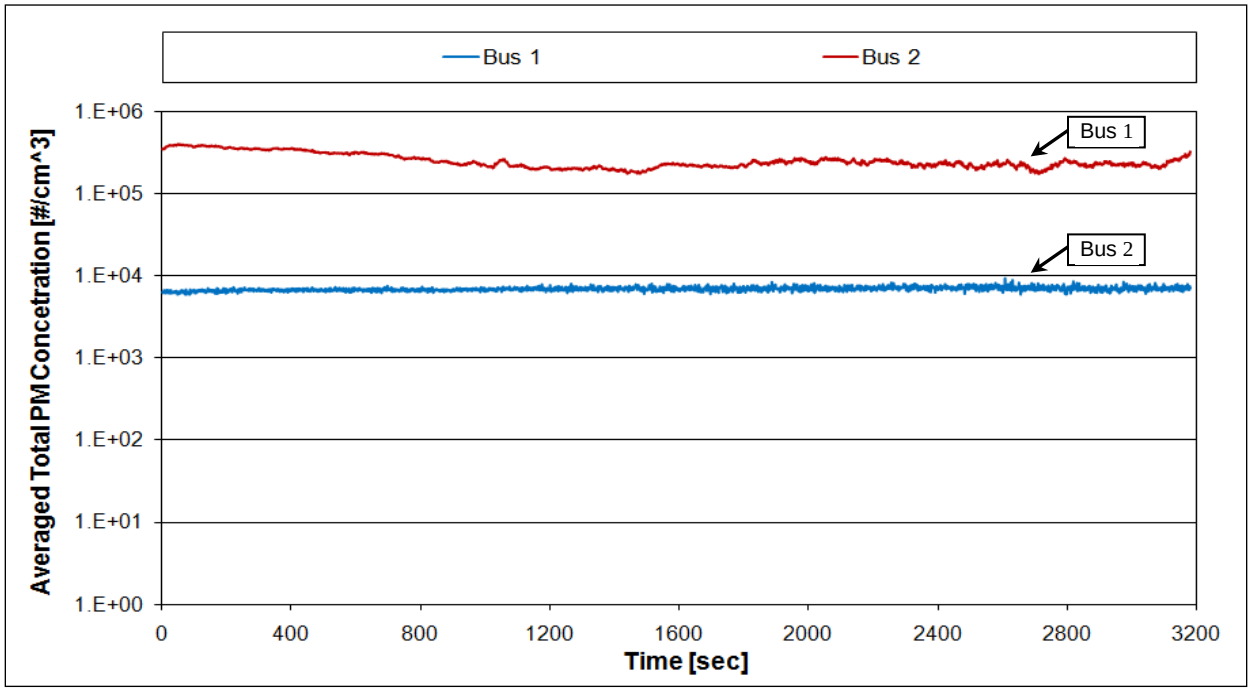

Figure 30 Total PM Concentration over Idle mode, Sampled from CVS tunnel, No dilution ratio corrections, EEPS

5.3.8 Ammonia emissions

Quantification of ammonia was not part of the work plan. However, analyzer interference issues experienced with the heated NO_x stream, hinted towards possible high ammonia levels

from the exhaust. Ammonia is believed to form salts of ammonia in the heated NO_x stream and deposit on the NO_x detectors.

WVU setup a raw ammonia measurement system to quantify the ammonia level using an Ecophysics CLD 844 CM hr analyzer. Since, the possibility of ammonia was realized late in the study, ammonia quantification could only be performed on bus 2.

Figure 31 represents the instantaneous ammonia concentration over a 30 MPH steady state cycle. An average ammonia concentration of 87 ppm with a maximum concentration of 230ppm was detected in the raw exhaust stream. Since the air-fuel ratio of the engine is constantly varied, the ammonia emissions also show high variations with peak associated with rich fuel-air mixtures. Similarly, high levels of ammonia emissions were also observed (Figure 32) over a 45MPH steady state cycle with an average concentration of 88 PPM and a maximum ammonia concentration of 280 ppm.

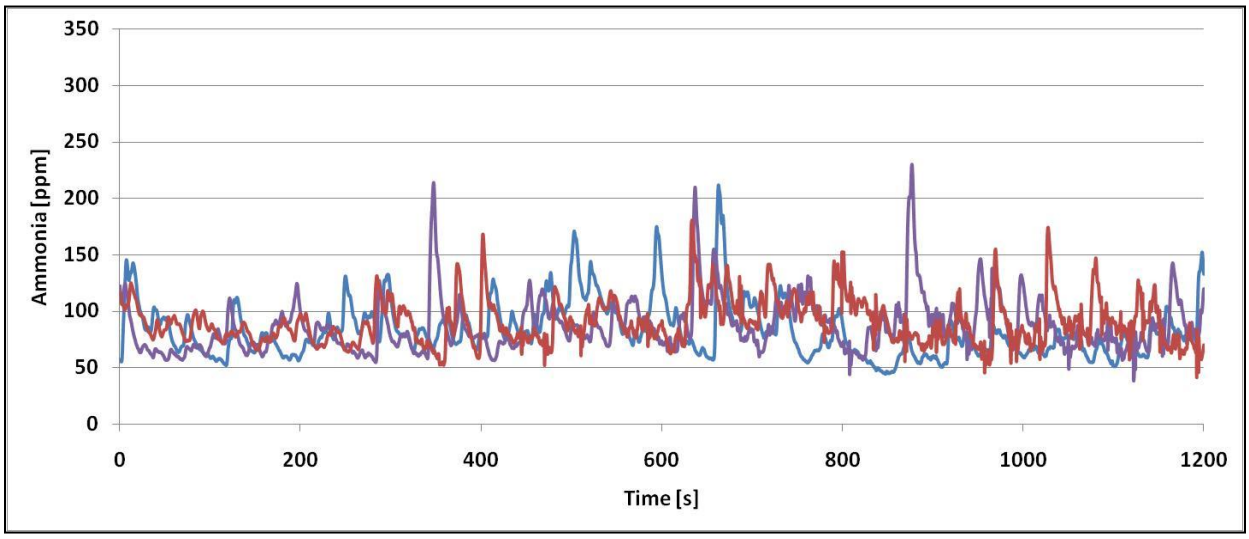

Figure 31 Ammonia concentrations over 30 MPH steady state

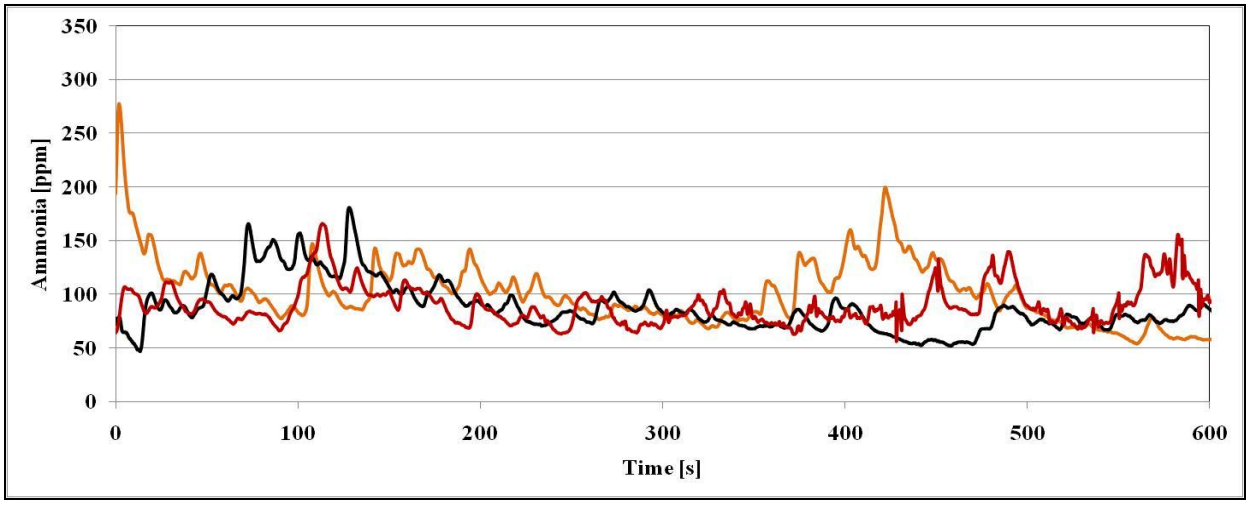

Figure 32 Ammonia concentrations over 45 MPH steady state

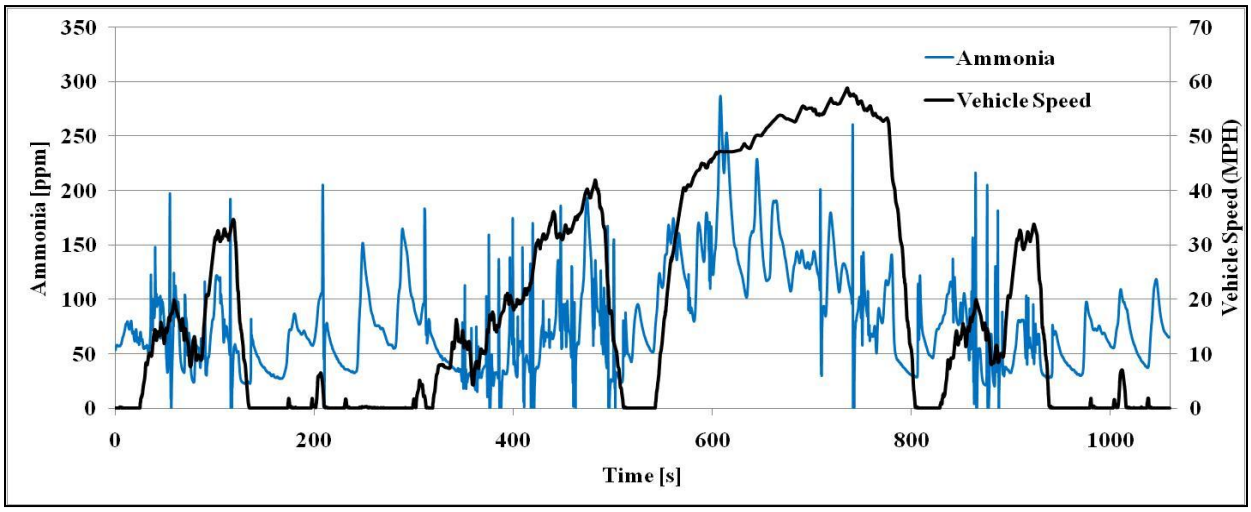

Figure 33 Ammonia concentrations over UDDS

Figure 33 represents the instantaneous ammonia concentration over the UDDS cycle. Average ammonia emissions of 75 ppm and a maximum concentration of 287 ppm were detected. Since, the production of ammonia is a catalytic process and depends on the presence of CO water and catalytic production of hydrogen, the emissions of ammonia cannot be directly related to the vehicle speed or engine load. Ammonia emissions are however closely related to the instantaneous air-fuel ratio and the exhaust temperature suitable for producing hydrogen as a result of water gas shift reaction.

A more detailed study relating 2010 CNG engines and its associated ammonia emissions should be performed to better understand the ammonia formation mechanism and its possible contribution to secondary PM formation.

6 CONCLUSIONS

The chassis dynamometer testing of two 3-way catalyst equipped 2010 compliant CNG transit buses were successfully carried out. As part of the work plan of the study, thermally denuded and non-denuded PM samples were collected for toxicity analysis purposes of which the analysis are still underway. The project also involved a extensive chemical speciation of exhaust, to quantify the levels of toxic air contaminants being emitted from the vehicles. The test matrix included transient testing over the UDDS cycle and a steady state testing over 45 MPH cruise and idle mode operation.

The regulated emissions results from the truck indicated very low levels of NO_x emissions, due to the presence of 3-way catalyst. The hydrocarbon emissions from both buses consisted almost entirely of methane. Both buses exhibited very low levels of PM emissions, however PM emissions from bus 2 during idle mode operation was 52% greater than bus 1 based on mass and over a magnitude greater based on particle number concentration.

Analysis of PAH and VOC emissions revealed concentrations of most target species below detection limits. The EC/OC emissions profile indicated a completely organic carbon fraction of PM. However, it is also to be noted that significant levels of EC was observed during the idle mode operation of bus 2.

Results of carbonyl emissions indicate the effectiveness of the TWC in reducing formaldehyde, acetaldehyde and other carbonyl species to levels close background concentrations. The results of metals and ions also indicate test concentrations close to background levels.

The results for ROS, DTT-DHBA assay and mutagenicity are awaited and will be further attached as an addendum to this report once available.

7 REFERENCES

1. Gautam, M., 1999, ‘Particlate Matter and NOx Emissions from In-use Heavy-duty Diesel Vehicles", World Truck Conference, May 2-4, 1999, Monterey, CA.
2. Kappanna, H., (2006). "Reduction of Toxic Air Contaminancts TACs and Particulate Matter Emissions from Heavy-duty Natural Gas Engines", M.S. Thesis Advisor, Prof. Mridul Gautam, Department of Mechanical and Aerospace Engineering, West Virginia University, May 2006, Morgantown, WV.
3. Englert, N., (2004). Fine particles and human health-a review of epidemiological studies. Toxicol. Lett. 149, 235-242.
4. Nakashima, K., Ishihara, S., Urano, K., and Murata, K., "A study on Lubricating Oil Flow into the Combustion chamber for the Top Ring with a Special Joint," SAE Paper 982441, 1998. National Institute for Occupational Safety and Health. "Carcinogenic effects of exposure to diesel exhaust." NIOSH Current Intelligence Bulletin 50. DHHS NIOSH Publication #88-116. Centers for Disease Control and Prevention, Atlanta, GA. 1988.
5. International Agency for Research on Cancer. "Diesel and gasoline engine exhausts and some nitroarenes. Vol. 46. Monographs on the Evaluation of Carcinogenic Risks to Humans. World Health Organization, IARC, Lyon, France. (1989).
6. US Environmental Protection Agency. Health Assessment Document for Diesel Engine Exhaust. USEPA EPA/600/8-90/057F. 01 May 2002. U.S. Environmental Protection Agency, Office of Research and Development, National Center for Environmental Assessment, Washington, DC. 2002.
7. Ayala, A., N.Y. Kado, R.A. Okamoto, B.A. Holmen, P.A. Kuzmicky, R. Kobayashi, and K.E. Stiglitz (2002). "Diesel and CNG Heavy-duty Transit Bus Emissions over Multiple Driving Schedules: Regulated Pollutants and Project Overview," SAE Transactions Journal of Fuels and Lubricants, 735-747
8. Ayala, A., M.E. Gebel, R.A. Okamoto, P.L. Rieger, N.Y. Kado, C. Cotter, and N. Verma, (2003). "Oxidation Catalyst Effect on CNG Transit Bus Emissions," SAE Technical Paper 2003-01-1900.
9. Gautam, M, Thiagarajan, S., Burlingame, T., Wayne, W.S., Clark, N., Carder, D., (2004). "Characterization of Exhaust Emissions from a Catalyzed Trap Equipped Natural Gas Fueled Transit Bus", 14th CRC On-Road Vehicle Emissions Workshop, March 29-3 1, 2004, San Diego
10. Gautam, M., Kappanna, H., Wayne, W.S., Carder, D., Oshinuga, A., Tadrous, T., Graham, L., (2006). "Controlling Nanoparticle and Toxic Emissions from Natural Gas-Fueled Transit Buses", 10th ETH Conference on Combustion Generated Nanoparticles, August 21st 23rd 2006.
11. Gautam, M., (2006). "Control of Toxics and Nanoparticle Emissions from CNG-Fueled, Heavy-duty Transit Buses", SCAQMD Conference on Ultrafine Particles: The Science, Technology and Policy Issues, April 30 - May 2, 2006, Los Angeles, Ca Invited

12. Holmen, A.B., Ayala, A., Kado, N., Okamoto, R., "ARB's Study of Emissions from "Late-Model" Diesel and CNG Heavy-duty Transit Buses: Preliminary Nanoparticle Measurement Results", 5th ETH conference on Nanoparticle Measurements, August 6-8, 2001, Zurich.

13. Holmen, A.B., and A. Ayala, (2002). "Ultrafine PM Emissions from Natural Gas, Oxidation-Catalyst Diesel and Particle-Trap Diesel Heavy-Duty Transit Buses," Environmental Science and Technology, 36: 5041-5050.

14. Lev-On, M., LeTavec, Cl, Uilein, J., Alleman, T., Lawson, D., Vertin, K., Thompson, G., Gautam, M., Wayne, S., Zielinska, B., Sagebiel, J., Chatterjee, S., and Hallstrom, K., (2001). "Chemical Speciation of Exhaust Emissions from Trucks and Buses Fueled on Ultra-Low Sulfur Diesel and CNG", SAE 2002-02-0432, SAE International Spring Fuels and Lubricants Conference, Reno, NV.

15. Nightingale, J. A., Maggs, R., Cullinan, P., Donnelly, L. E., Rogers, D. F., Kinnersley, R., Fan, C. K., Barnes, P. J., Ashmore, M., and Newman-Taylor, A. 2000. Airway inflammation after controlled exposure to diesel exhaust particulates. American Journal of Respiratory Critical Care Medicine, 162, 161-166.

16. Nordenhall, C., Pourazar, J., Blomberg, A., Levin, J. 0., Sandstrom, T., and Adelroth, E. 2000. Airway inflammation following exposure to diesel exhaust: A study of time kinetics using induced sputum. Eur. Respir. J. 15, 1046-1051.

17. Rudell, B., Blomberg, A., Helleday, R., Ledin, M. C., Lundback, B., Stjernberg, N., Horstedt, P., and Sandstrom, T. 1999. Bronchoalveolar inflammation after exposure to diesel exhaust: Comparison between unfiltered and particle trap filtered exhaust. Occup. Environ. Med. 56, 527-534.

18. Salvi, S., Blomberg, A., Rudell, B., Kelly, F., Sandstrom, T., Holgate, S. T., and Frew, A. 1999. Acute inflammatory responses in the airways and peripheral blood after short-term exposure to diesel exhaust in healthy human volunteers. American Journal of Respiratory Critical Care Medicine 159, 702-709.

19. Stenfors, N., Nordenhall, C., Salvi, S. S., Mudway, I., Soderberg, M., Blomberg, A., Helleday, R., Levin, J. 0., Holgate, S. T., Kelly, F. J., Frew, A. J., and Sandstrom, T. 2004. Different airway inflammatory responses in asthmatic and healthy humans exposed to diesel. European Respiratory Journal 23, 82-86.

20. Seagrave, J., Gigliotti, A., McDonald, J., Seilkop, S., Whitney, K., Zielinska, B., Mauderly, J., 2005, "Composition, Toxicity, and Mutagenicity of Particulate and Semivolatile Emissions", Toxicological Sciences 2005 871 :232-241; doi: 10.1 093/toxsci/kfi230

21. Brauer, M., Hoek, G., van Vliet, P., Meliefste, K., Fischer, P. H., Wijga, A., Koopman, L. P., Neijens, H. J., Gerritsen, J., Kerkhof, M., Heinrich, J., Bellander, T., and Brunekreef, B., (2002). Air pollution from traffic and the development of respiratory infections and asthmatic and allergic symptoms in children. Am. J. Respir. Crit. Care Med. 166, 1092-1098. Referenced from: Seagrave et al., (2005).

22. Brunekreef, B., Janssen, N. A., de Hartog, J., Harssema, H., Knape, M., and van Vliet, P., (1997). Air pollution from truck traffic and lung function in children living near motorways, Epidemiology, 8, pp. 98-303. Referenced from: Seagrave et al., (2005).

23. Finkelstein, M. M., (2003). Mortality and indicators of traffic-related air pollution, Lancet 361, 430. Referenced from: Seagrave et al., (2005).

24. McCormick, R. L., Graboski, M. S., Alleman, T. L., and Yanowitz, J., (2000). Idle emissions from heavy-duty diesel and natural gas vehicles at high altitude. J. Air Waste Manag. Assoc. 50, 1992-1998.

25. Lapin, C. A., Gautam, M., Zielinska, B., Wagner, V. O., and McClellan, R. O., (2002). Mutagenicity of Emissions from a Natural Gas Fueled Truck. Mutation Research 519, 205-209.

26. Sakurai, H., Tobias, H. J., Park, K., Zarling, D., Docherty, S., Kittelson, D. B., McMurry, P. H., and Ziemann, P. J. 2003. On-Line Measurements of Diesel Nanoparticle Composition and Volatility, Atmospheric Environment 379-10: 1199-1210.

27. McDonald, J.D., Eide, I., Seagrave, J., Zielinska, B., Whitney, K., Lawson, D.R., and Joe L. Mauderly, J.L., 2004, "Relationship between Composition and Toxicity of Motor Vehicle Emission Samples", Environmental Health Perspectives Volume 112, Number 15, November 2004.

28. Liu, Y-Q, Keane, M., Ensell, M., W Miller, W., Kashon, M., Ong, T., Mauderly, J., Lawson, D., Gautam, M., Zielinska, B., Whitney, K., Wallace, W., (2005). "In-Vitro Genotoxicity of Exhaust Emissions of Diesel and Gasoline Engine Vehicles Operated on a Unified Driving Cycle", Journal of Environmental Monitoring, 7:60-66.

29. Whitney KA. 2000. Collection of In-Use Mobile Source Emission Samples for Toxicity Testing. SwRI document 08.02602. Final report to the National Renewable Energy Laboratory. Golden, CO:National Renewable Energy Laboratory.

30. Seagrave, J. C., McDonald, J. D., Gigliotti, A. P., Nikula, K. J., Seilkop, S. K., Gurevich, M., and Mauderly, J. L. 2002. Mutagenicity and in vivo toxicity of combined particulate and semivolatile organic fractions of gasoline and diesel engine emissions. Toxicological Science 70, 212-226.

31. Zielinska B, Sagebiel J, McDonald J, Whitney K, Lawson DR. 2004. Emission rates and comparative composition of in-use diesel and gasoline fueled vehicle emissions. Journal of Air Waste Management Assocation 54:1138-1150.

32. McMillian, M.H., Cui, M., Gautam, M., Keane M., Ong, T., Wallace, W., Robey, E., "Mutagenic Potential of Particulate Matter from Diesel Engine Operation on Fischer-Tropsch as a Function of Engine Operating Conditions and Particulate Size," SAE 2002-01-1699, 2002.

33. Bagley, S. T., Baumgard, K. J., Gratz, L.D. Johnson, J.H., and Leddy, D.G., "Characterization of Fuel and After-treatment Device Effects on Diesel Emissions," Health Effects Institute Research Report No. 76, (1996).

34. Yuan, D., Zhou, W., and Ye, S., "Effect of Leaded and Unleaded Gasoline on the Mutagenicity of Vehicle Exhaust Particulate Matter," Journal of Environmental Pathology, Toxicology and Oncology, Vol. 19, pp. 4 1-48, 2000.

35. Okamoto, R.A., Kado, N.Y., Kuzmicky, P.A., Ayala, A., and Kobayashi, R. "Unregulated emissions from Compressed Natural Gas CNG Transit Buses Configured with and without oxidation Catalyst," Environmental Science & Technology, vol.40, No. 1, 2006.

36. Kado, N., Okamoto, R.A., Kuzmicky, P.A., Kobayashi, R., Ayala, A., Gebel, M.E., Rieger, P.L., Maddox, C., and Zafonte L., "Emission of Toxic Pollutants from Compressed Natural Gas and Low sulfur Diesel-Fueled Heavy Duty Transit Buses Tested over Multiple Driving Cycles," Environmental Science & Technology, Vol. 39, No. 19, (2005).

37. Li, H., Karim, G.A., and Sohrabi, A., "Examination of the Oil Combustion in a SI Hydrogen Engine," SAE 2004-01-2916, (2004).

38. Lee, S.J., Yi, H.S, Kim, E.S., "Combustion Characteristics of Intake Port Injection Type Hydrogen Fueled Engine," International Journal of Hydrogen Energy, Vol. 20, No. 4, pp 317-322, (1995).

39. Miller A.L., Stipe, C.B., Habjan, M.C., and Ahlstrand, G.G., "The Role of Lubrication Oil in Particulate Matter Emissions from a Hydrogen Engine," NIOSH, Pending for publication, 2006.

40. Kittelson, D., Abdul-Khalek, I., "Formation of Nanoparticles During Exhaust Dilution," EFI Members Conference: "Fuels, Lubricants Engine & Emissions", January 18-20, (1999).

41. Froelund, K., Owens, W.C., Frame, E., Buckingham, J.P., Garbak, J., Tseregounis, S., and Jackson, A., "Impact of Lubrication Oil on Regulated Emissions of a Light-Duty Mercedes-Benz OM611 CDI Engine," SAE 2001-01-1901, (2001).

42. Anderson, J., Preston, H., Warrens, C., and Brett, P., "Fuel and Lubricant Effects on Nucleation Mode Particles Emissions from a Euro III Light Duty Diesel Vehicle," SAE 2004-01-1989, (2004).

43. Jung, H., Kittelson D.B., and Zachariah, M.R., "The Influence of the Engine Lubricating Oil on Diesel Nanoparticle Emissions and Kinetics of Oxidation," SAE 2003-01-3179, (2003).

44. Essig, G., Kamp, H., and Wacker, E., "Diesel Engine Emissions Reduction - The Benefits of Low Oil Consumption Design," SAE Paper 900591, (1990).

45. Furuhama, S., Hiruma, M., "Unusual Phenomena in Engine Oil Consumption," Journal of ASLE, Vol. 36, No. 10, pp. 599-606, (1979).

46. Li, H., Karim, G.A., "Exhaust Emissions form an SI Engine Operating on Gaseous Fuel Mixtures Containing Hydrogen," International Journal of Hydrogen Energy, Vol. 30, pp. 1491-1499, (2005).

47. Thirouard, B., Tian, T., "Oil Transport in the Piston Ring Pack Part I: Identification and Characterization on the Main Oil Transport Routes and Mechanisms," SAE 2003-01-1952, 2003.

48. Rabute, R., Tian, T., "Challenges Involved in Piston Top Ring Design for Modern SI Engines," Transaction of the ASME, Vol. 123, April 2003, 2003.

49. Health Effects Institute. "Diesel emissions and lung cancer: a special report of the Institute's diesel epidemiology expert panel." HEI, Boston, MA; www.healtheffects.org/pubs.htm

(1999). Herbst, H.M., Priebsch, H.H., "Simulation of Piston Ring Dynamics and Their Effect on Oil Consumption," SAE 2000-01-0919, (2000).

50. Furuhama, S., Hiruma, M., Yoshida, H., "An Increase of Engine Oil Consumption at High Temperature of piston and Cylinder," SAE Paper 810976, (1981).
51. Icoz, T., Dursurikaya, Z., "Experimental Investigation of Oil Accumulation in Second Land of Internal Combustion Engines," Transaction of the ASME, Vol. 127, January, (2005).
52. Piao, Y., Gulwadi, S.D., "Numerical Investigation of the Effects of Axial Cylinder Bore Profiles on Piston Ring Radial Dynamics," Journal of Engineering for Gas Turbines and Power, ASME, October 2003, Vol. 125, 2003.
53. Gautam, M., Thiruvengadam, A., Besch, M. C., Ardanese, R., Ardanese, M., Thiagarajan, M., et al. (2009). PM size distrubution from a DPF-SCR equipped 2010 compliant heavy-duty diesel engine during NTE zone opeartion. 19th CRC On-Road Vehicle Emissions Workshop. San Diego.
54. Heeb, N.V., Forss, A.M., Bruhlmann, S., Luscher, R., Saxer, C.J. and Hug, P., (2006). Three-way catalyst-induced formation of ammonia: velocity and acceleration dependent emission factors. Atmospheric Environment, Vol. 40, pp. 5986-5997
55. Heeb, N. V., Saxer, C. J., Forss, A.-M., & Bruhlmann, S. (2006). Correlation of hydrogen, ammonia and nitrogen monoxide emissions of gasoline-fueled Euro-3 passenger cars at transient driving. Atmospheric Environment, 3750-3763.
56. Plerson, W.R., Brachaczek, W.W., 1983. Emissions of Ammonia and Amines from Vehicles on the Road. Environ. Sci. Technol., Vol. 17, pp. 757-760.
57. Fitz, D., William, A., Welch, W.A., October 2001. Quantification of Uncertainties in Continuous Measurement Systems for Low NOx Emissions from Stationary Sources. Final Report, 01-AP-18491- 01-DFR for the California Institute for Energy Efficiency.
58. Nakatani, S., Yoshimura, T., Mori, Y., et al., 2004. Development of a Real-time NH3 Gas Analyzer Utilizing Chemi-luminescence Detection for Vehicle Emission Measurement. SAE Technical Paper No. 2004-01-2907.
59. Durbin, T.D., Wilson, R.D., Norbeck, J.M., Miller, J.W., Huai, T., Rhee, S.H., 2002. Estimates of the emission rates of ammonia from light-duty vehicles using standard chassis dynamometer test cycles. Atmospheric Environment, Vol. 26, pp. 1475-1482.
60. Mohn, J., Forss, A.M., Bruhlmann, S., Zeyer, K., Luscher, R., Emmenegger, L., Novak, P., Heeb, N., 2004. Time-resolved ammonia measurement in vehicle exhaust. Int. J. Environment and Pollution, Vol. 22, No. 3, pp. 342-356.
61. Heeb, N.V., Saxer, C.J., 2005. Ammoniak-Emissionen von benzin-betriebenen EURO-3 Personenwagen, CI-MS-Untersuchungen an 12 G-Kat-Fahrzeugen der Jahrgange 2000-2003 (EURO-3). Report. Organic Chemistry Laboratory, EMPA Dubendorf, Switzerland.
62. Ardanese, R., Ardanese, M., et al. 2008. Control of NOx and PM Emissions form SCR-equipped 2010 Compliant Heavy Duty Diesel Engines over Different Engine-Out Calibrations. PhD Dissertation, West Virginia University.

63. Adams, T., 2008. Development of an Open Loop Fuzzy Logic Urea Dosage Controller for Use with an SCR Equipped HDD Engine. Master Thesis, West Virginia University.

64. Bedick, C., 2009. Optimization of a Retrofit Urea-SCR System. PhD Dissertation, West Virginia University.

65. Leippe, G., Lenzen, B., Spurk, P., Fabinski, W., Moede, M., Pongraz, H., Schindler W., and Schiefer, E., 2004. A New System for Measuring the Nitrogen Components N2O, NH3, NO and NO2 Downstream of DeNOX Catalytic Converters. MTZ worldwide, Vol. 65, Issue 5, pp. 392-399.

66. Ciardelli, D., Nova, I., Tronconi, E., et al., 2007. Combined use of a mass-spectrometer and a UV analyzer in the dynamic study of NH3-SCR for diesel exhaust after-treatment. Topics in Catalysis, Vols. 42-43, pp. 161-164.

67. Lenaers, G., Van Poppel, M., 2006. On-board real life ammonia measurement for vehicles with recent emission control technology. Vito, Flemish Institute for Technological Research. Belgium.

68. Baronick, J.D., Heller, B., Lach, G., et al., 2001. Evaluation of an UV Analyzer for NOx Vehicle Emission Measurement. SAE Technical Paper No. 2001-01-0213.

69. Schiefer, E., Schindler, W., Schimpl, H., 2000. Study of Interferences for ULEV-CVS Measurement, Related to the Complete Measuring System, Discussion of Error Sources, Cross-Sensitivity and Adsorption. SAE Technical Paper No. 2000-01-0796.

70. UNECE, Subgroup Transportation, 2010. Draft Ammonia (NH3) measurement procedure. Working Paper No. WLTP-DTP-02-07.

71. Wu, Y., Carder, D., Shade, B., Atkinson, R., Clark, N., & Gautam, M. (2009). A CFR1065-Compliant Transportable/On-Road Low Emissions Measurement Laboratory With Dual Primary Full-Flow DIlution Tunnels. Milwaukee, Wisconsin USA.

72. Desert Research Institute. (2000). *Thermal/Optical Reflectance Carbon Analysis-DRI STANDARD OPERATING PROCEDURE.* Reno, NV, USA: Desert Research Institute.

73. Peterson, M. R., & Richards, M. H. *Thermal-Optical-Transmittance Analysis for Organic, Elemental, Carbonate, Total Carbon, and OCX2 in PM2.5 by the EPA/NIOSH Method - #83.* Research Triangle Park, NC USA: Research Triangle Institute.

74. Herner, J. D.; Hu, S.; Robertson, W. H.; Huai, T.; Collins, J. F.; Dwyer, H.; Ayala, A., Effect of Advanced Aftertreatment for PM and NOx Control on Heavy-Duty Diesel Truck Emissions. Environ Sci Technol 2009, 43, (15), 5928-5933.

75. Ayala, A.; Kado, N. Y.; Okamoto, R. A.; Holmén, B. A.; Kuzmicky, P. A.; Kobayashi, R.; Stiglitz, K. E., Diesel and CNG heavy-duty transit bus emissions over multiple driving schedules: Regulated pollutants and project overview. SAE Transactions Journal of Fuels and Lubricants 2002, 735-747.